Remote sensing of phytoplankton size classes on the northeast U.S. continental shelf

Kyle J. Turner

Email: k.turner00@ccny.cuny.edu

NOAA OCCG Seminar
January 6, 2021

THE
UNIVERSITY
OF RHODE ISLAND
GRADUATE SCHOOL
OF OCEANOGRAPHY

Acknowledgements

NOAA
Northeast Fisheries Science Center
Narragansett, RI


Kim Hyde


Ryan Morse

URI
Graduate School of Oceanography
Narragansett, RI


Colleen Mouw


Audrey Ciochetto

Joint Polar Satellite System (JPSS) Proving Ground and Risk Reduction Program

Phytoplankton size

Phytoplankton cell size influences:

- photosynthesis[1]
- nutrient uptake[2]
- maximum growth rate[3]
- light absorption[4,5]
- carbon export[6,7]
- trophic energy transfer[8]

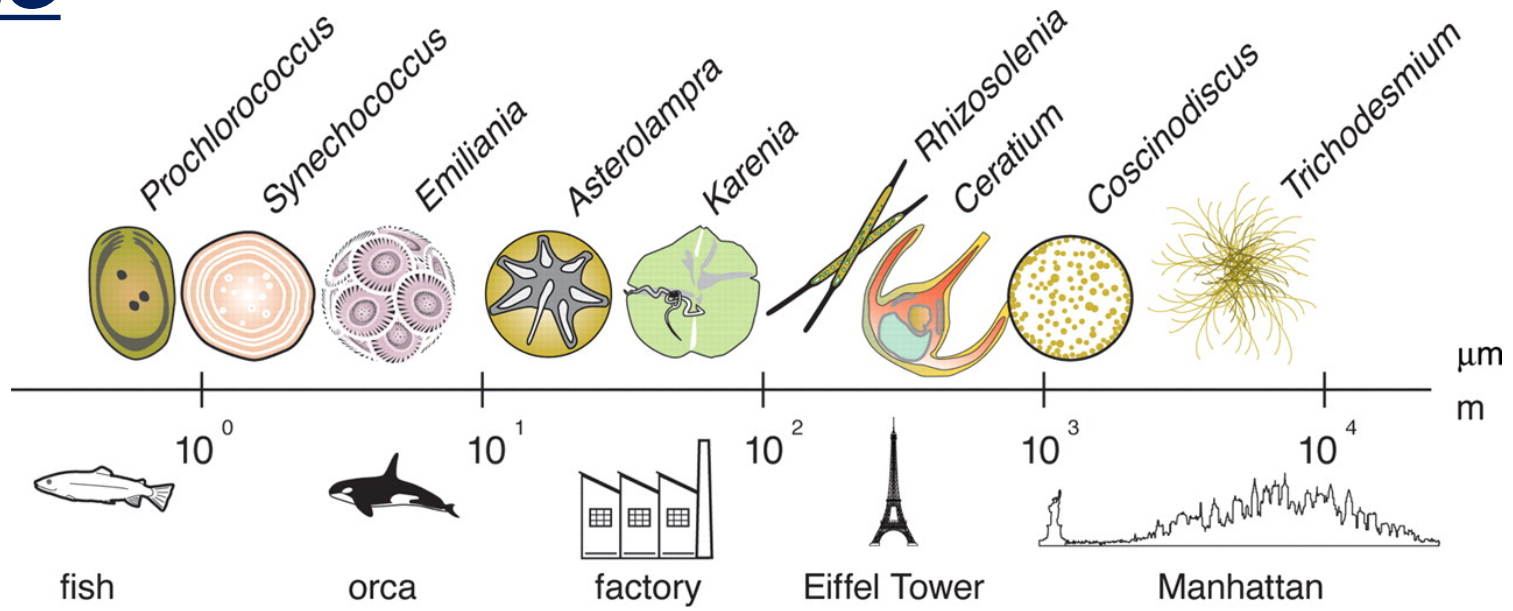

Finkel et al. (2010)

Three conventional size classes (PSCs) (Sieburth, 1978):

- **Pico**plankton (0.2-2 μm)
- **Nano**plankton (2-20 μm)
- **Micro**plankton (20-200 μm)

[1]Uitz et al. (2008), [2]Raven (1998), [3]Marañon (2015), [4]Ciotti et al. (2002), [5]Bricaud (2004), [6]Guidi et al. (2009), [7]Mouw et al. (2016), [8]Boyce et al. (2015)

Satellite PSC algorithms

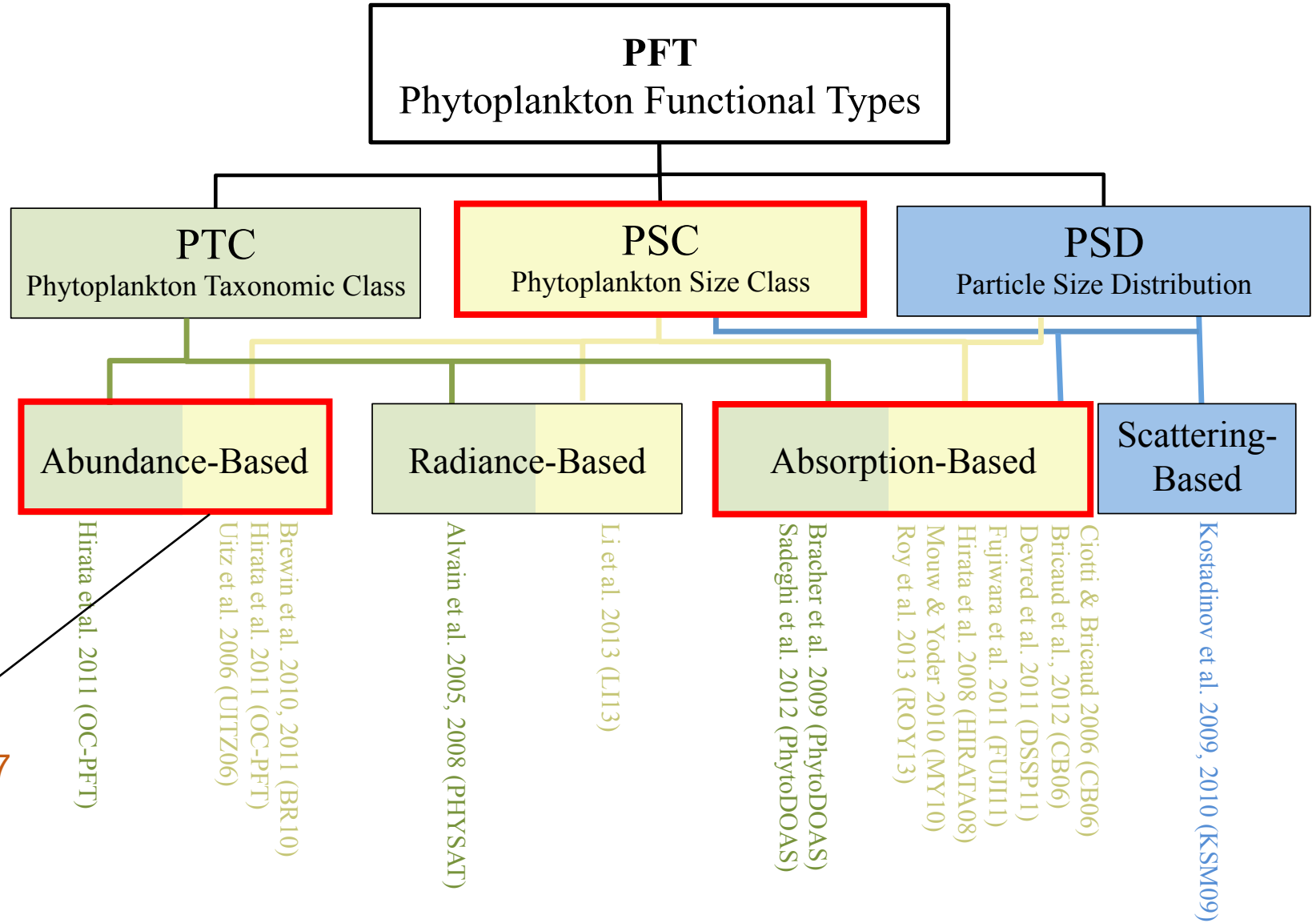

Brewin et al. 2015; 2017
Moore & Brown 2020

[Include SST]

Mouw et al. (2017)

Northeast U.S. continental shelf (NES)

NOAA (2020)

- **Highly productive**, temperate marine ecosystem
- Supports many **economically important fisheries**
- **Undergoing rapid warming**[1] which has been connected to changes in phytoplankton bloom dynamics[2] and shifts in the distributions of fish and other marine species[3]

[1]Pershing et al. (2015), [2]Hunter-Cevera et al. (2016), [3]Kleisner et al. (2017)

Motivation

Evaluate the performance of existing satellite PSC algorithms in the NES region and determine whether they can be **optimized for regional application**

Goal: Generate improved PSC imagery products for **long-term time series investigations** and integration into **regional ecosystem modeling and fisheries management**

Questions

1. Does re-parameterization of abundance-based PSC models using a local *in situ* data set improve performance in the NES?

2. Can incorporating *SST* into an abundance-based model framework improve model performance in the NES?

3. How do abundance-based and absorption-based algorithms compare in their estimations of PSCs in the NES?

In situ data

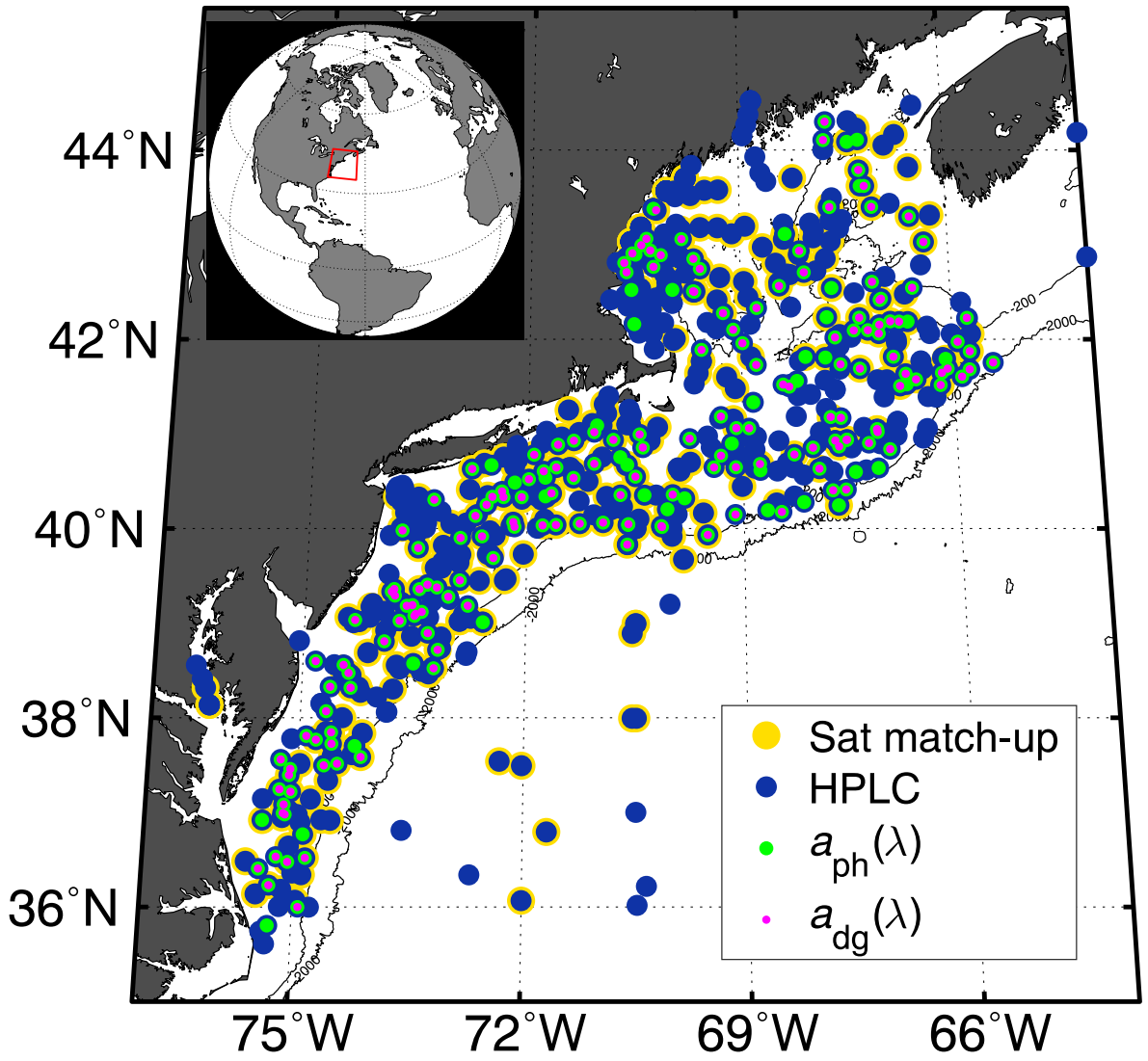

Bathymetry data from GEBCO 2019 (https://www.gebco.net/)

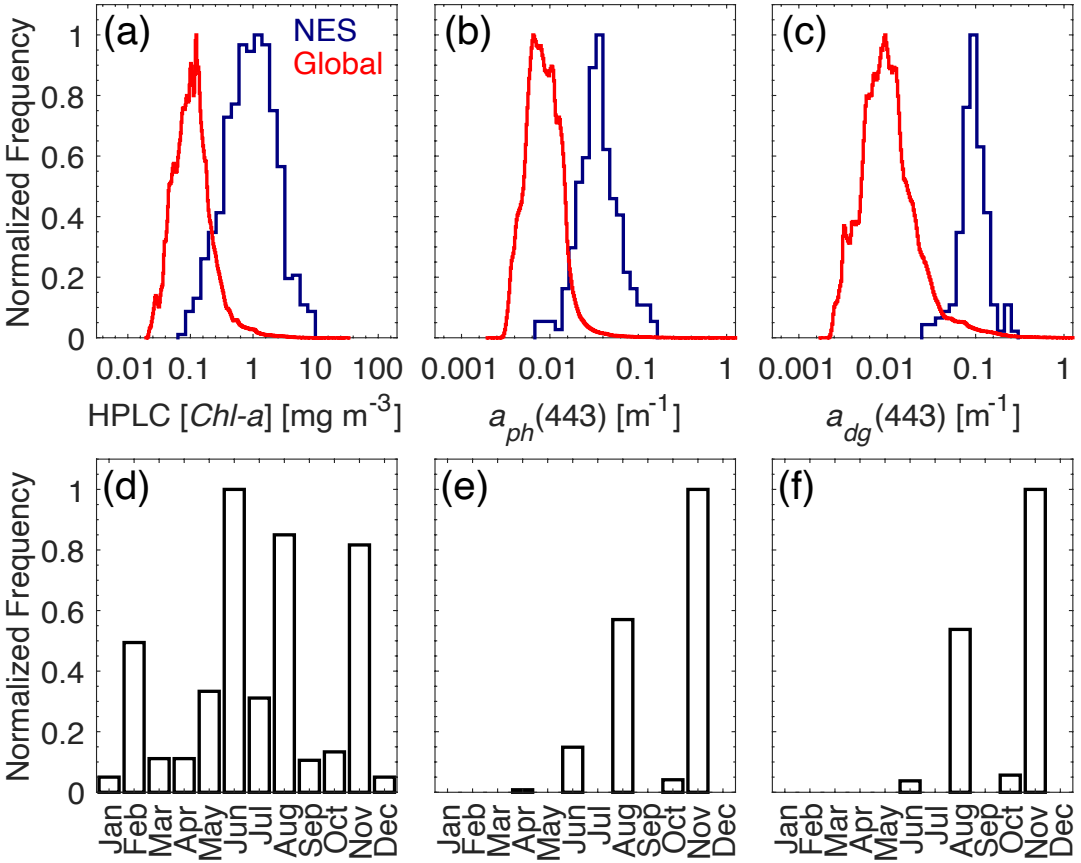

- Downloaded from NASA's **SeaBASS** data repository [https://seabass.gsfc.nasa.gov/]
- Samples collected on Summer and Fall 2018 NOAA Ecosystem Monitoring (**EcoMon**) surveys

EcoMon surveys

Participated in five cruises:

Summer 2018, Fall 2018, Spring 2019,
Summer 2019, Fall 2019

CTD-Rosette deployment

Radiometry

Photo credit: Jerry Prezioso

Spring 2019 cruise track

Continuous flow-through optics, phytoplankton imaging, and discrete optical sampling

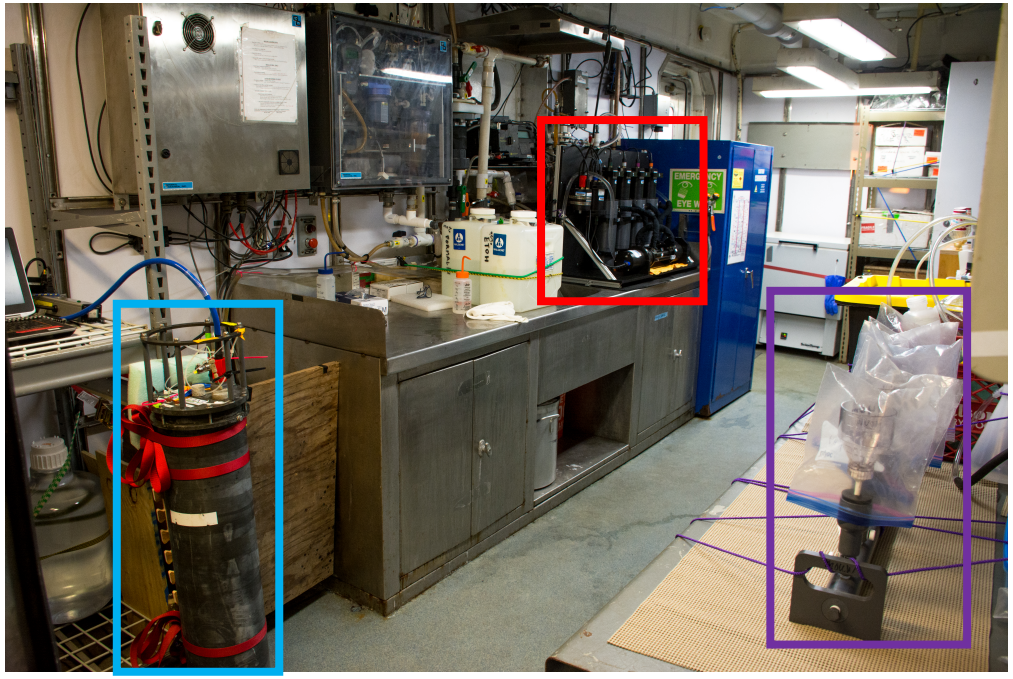

Satellite data

- $R_{rs}(\lambda)$, [*Chl-a*], $a_{ph}(\lambda)$, and $a_{dg}(\lambda)$ from the European Space Agency's **Ocean Colour – Climate Change Initiative (OC-CCI) version 4.2** (1997-2019)[1] [https://esa-oceancolour-cci.org/]
  - Match-ups with *in situ* data determined as median of 3x3 pixel box centered on sampling location (same day)
    - 368 HPLC, 123 $a_{ph}(\lambda)$, 99 $a_{dg}(\lambda)$ match-ups

https://esa-oceancolour-cci.org/

- *SST* from **Multi-scale Ultra-high Resolution analysis (MUR) version 4.1** (2002-2019)[2] [https://podaac.jpl.nasa.gov]
  - Daily, gap-filled, 1-km resolution
  - Matched with all *in situ* samples in time and space

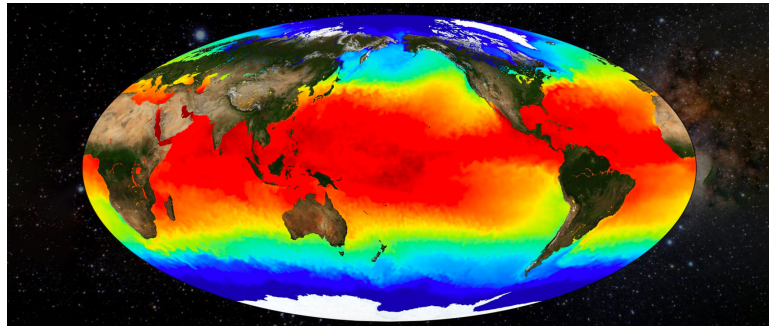

https://podaac.jpl.nasa.gov/

[1]Sathyendranath et al. (2019), [2]Chin et al. (2017)

Data partitioning

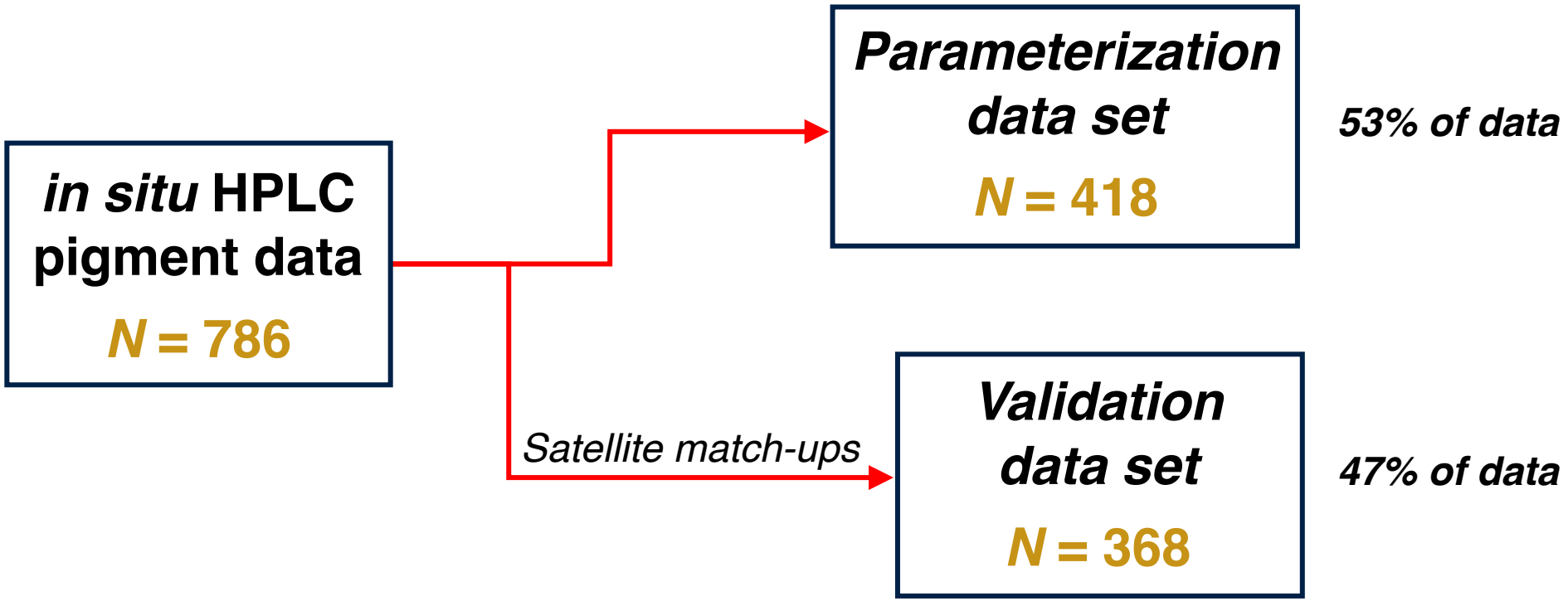

Statistical metrics

- **Mean Absolute Error (*MAE*):** $$MAE = \frac{1}{N}\sum_{i=1}^{N}|M_i - O_i|$$

- **Mean Bias (δ):** $$\delta = \frac{1}{N}\sum_{i=1}^{N}(M_i - O_i)$$

N represents the number of samples

M represents the modeled value (i.e., satellite estimate)

O represents the observed value (i.e., *in situ* measurement)

- **Pearson correlation coefficient (*r*):** MATLAB function *corr.m*

- **Slope of Type-II linear regression (*S*):** MATLAB function *lsqfitgm.m*

Estimation of PSCs from HPLC pigments

Diagnostic Pigment Analysis (DPA)[1,2,3,4,5]

$$C_{DP} = \sum_{i=1}^{7} W_i \, P_i,$$

[***W***] = pigment-specific weighting coefficients

[***P***] = { [*Fuco*], [*Perid*], [*Hex-fuco*], [*But-fuco*], [*Allo*], [*TChl-b*], [*Zea*] }

$$F_{micro} = \frac{\sum_{i=1}^{2} W_i \, P_i - W_1 P_{1,nano}}{C_{DP}}$$

$$F_{nano} = \frac{\sum_{i=3}^{5} W_i \, P_i + W_1 P_{1,nano}}{C_{DP}}$$

$$F_{pico} = \frac{\sum_{i=6}^{7} W_i \, P_i}{C_{DP}}$$

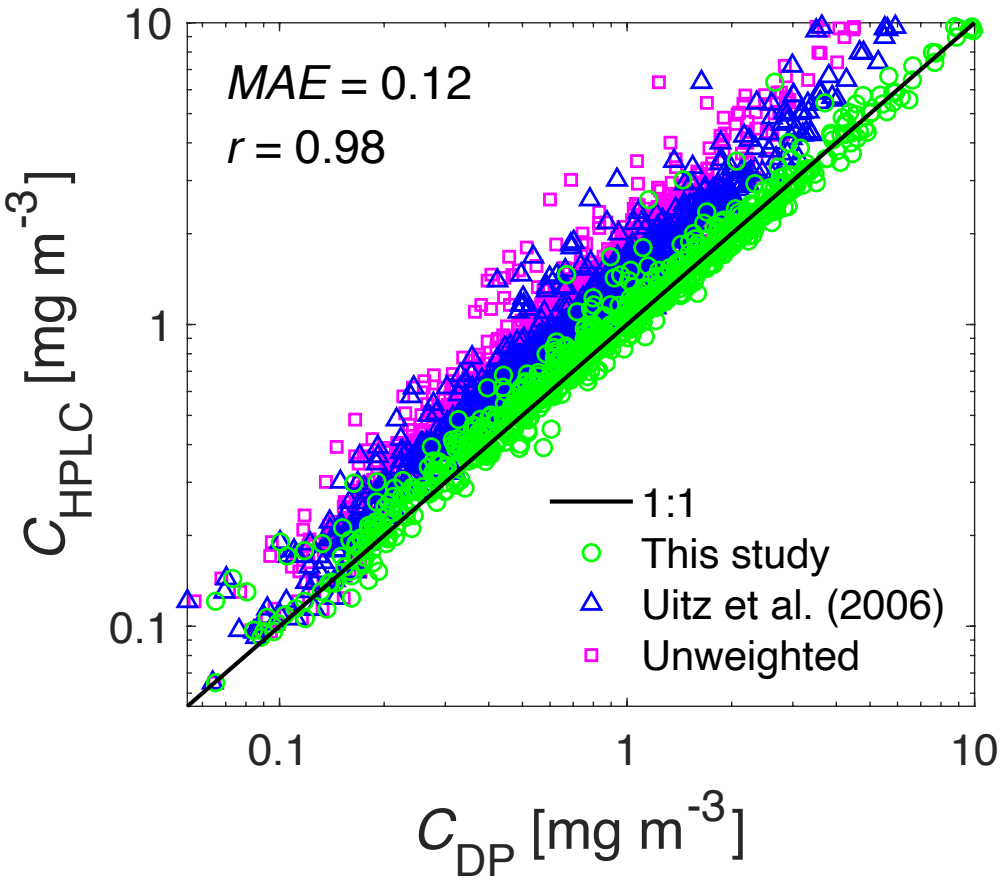

Uitz et al. (2006): *MAE* = 0.47, *r* = 0.96

Unweighted: *MAE* = 0.62, *r* = 0.96

[1]Vidussi et al. (2001), [2]Claustre (2005), [3]Uitz et al. (2006), [4]Devred et al. (2011), [5]Brewin et al. (2015)

Estimation of PSCs from HPLC pigments

Diagnostic Pigment Analysis (DPA)[1,2,3,4,5]

$$C_{DP} = \sum_{i=1}^{7} W_i \, P_i,$$

[***W***] = pigment-specific weighting coefficients

[***P***] = { [*Fuco*], [*Perid*], [*Hex-fuco*], [*But-fuco*], [*Allo*], [*TChl-b*], [*Zea*] }

$$C_{micro} = F_{micro} C_{HPLC}$$

$$C_{nano} = F_{nano} C_{HPLC}$$

$$C_{pico} = F_{pico} C_{HPLC}$$

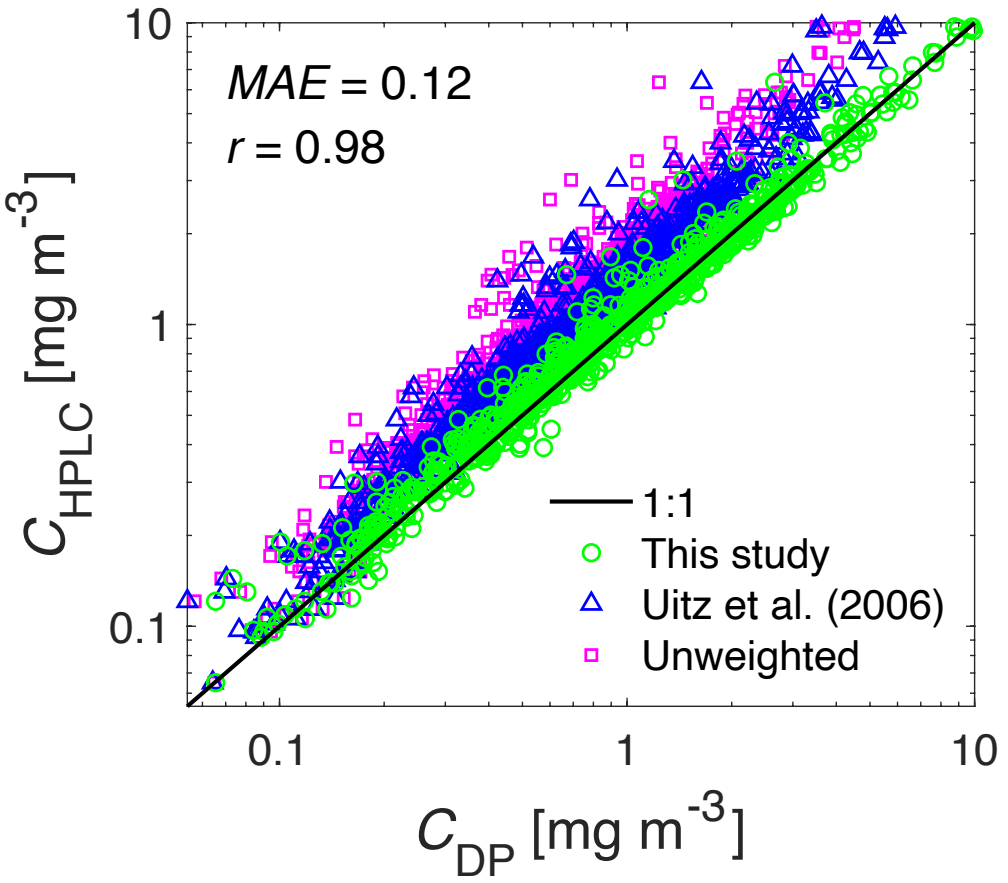

Uitz et al. (2006): *MAE* = 0.47, *r* = 0.96

Unweighted: *MAE* = 0.62, *r* = 0.96

[1]Vidussi et al. (2001), [2]Claustre (2005), [3]Uitz et al. (2006), [4]Devred et al. (2011), [5]Brewin et al. (2015)

Abundance-based algorithms

Estimate the fractional contribution of PSCs based on total [Chl-a]

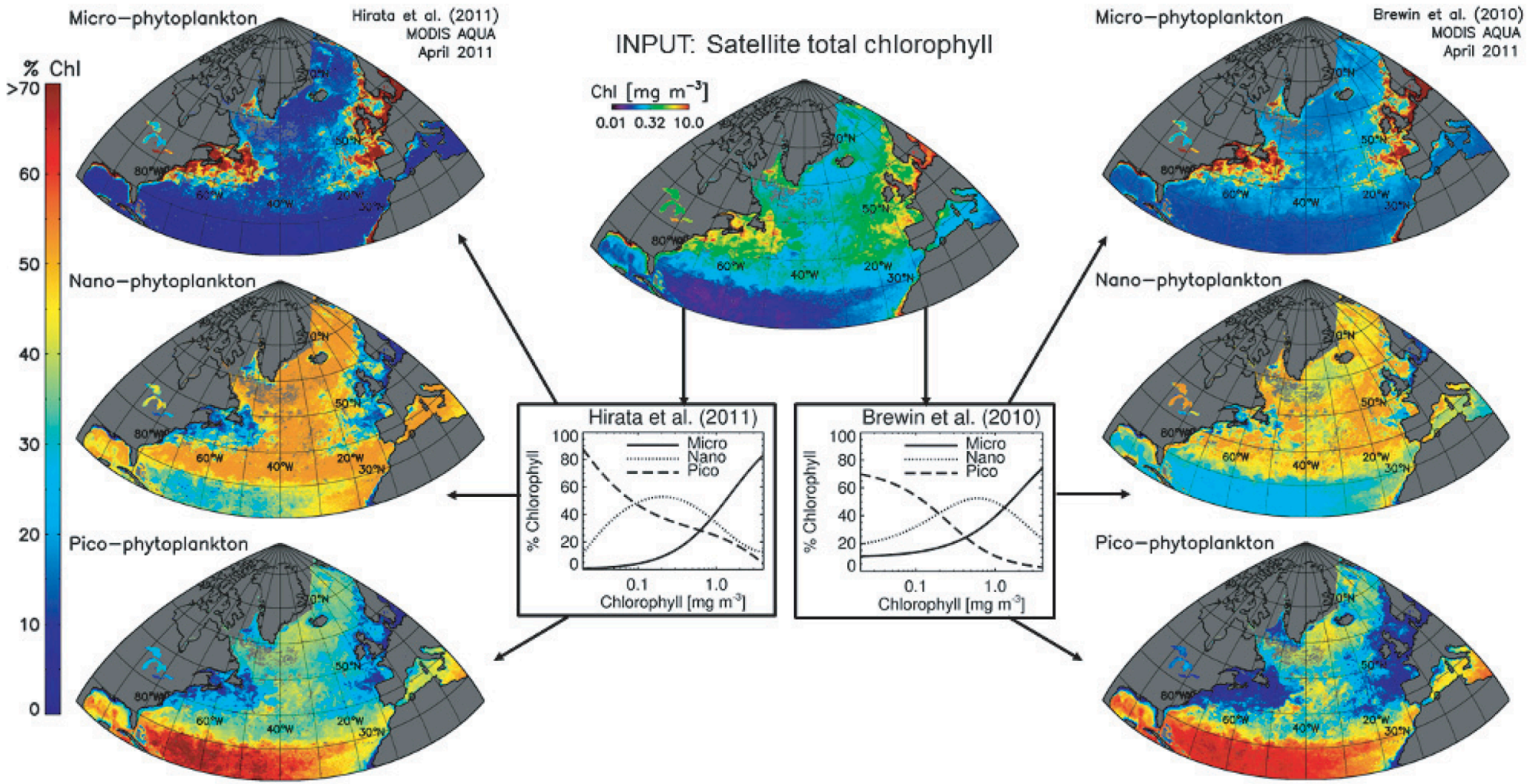

Abundance-based algorithms

Brewin et al. (2010) [B10]:

$$F_{pico,nano} = \frac{C^m_{pico,nano}\left[1 - exp\left(-\frac{D_{pico,nano}}{C^m_{pico,nano}}[Chl\text{-}a]\right)\right]}{[Chl\text{-}a]}$$

$$F_{pico} = \frac{C^m_{pico}\left[1 - exp\left(-\frac{D_{pico}}{C^m_{pico}}[Chl\text{-}a]\right)\right]}{[Chl\text{-}a]}$$

Model parameters:

$\boldsymbol{C^m_{pico}}$ & $\boldsymbol{C^m_{pico,nano}}$ = maximum chlorophyll concentration of size class

$\boldsymbol{D_{pico}}$ & $\boldsymbol{D_{pico,nano}}$ = fraction of size class as total [*Chl-a*] tends toward zero

Hirata et al. (2011) [H11]:

$$F_{micro} = [a_1 + exp(a_2 X + a_3)]^{-1}$$

$$F_{pico} = [b_1 + exp(b_2 X + b_3)]^{-1}$$

where

X = log10([*Chl-a*])

Re-parameterized Brewin model: [**B-NES**]

Re-parameterized Hirata model: [**H-NES**]

Brewin et al. (2010): [**B10**]

Brewin et al. (2015): [**B15**]

Brewin et al. (2017): [**B17**]

Devred et al. (2011): [**D11**]

Hirata et al. (2011): [**H11**]

Moore and Brown (2020): [**MB20**]

Brewin model framework

Hirata model framework

Comparison of abundance-based models

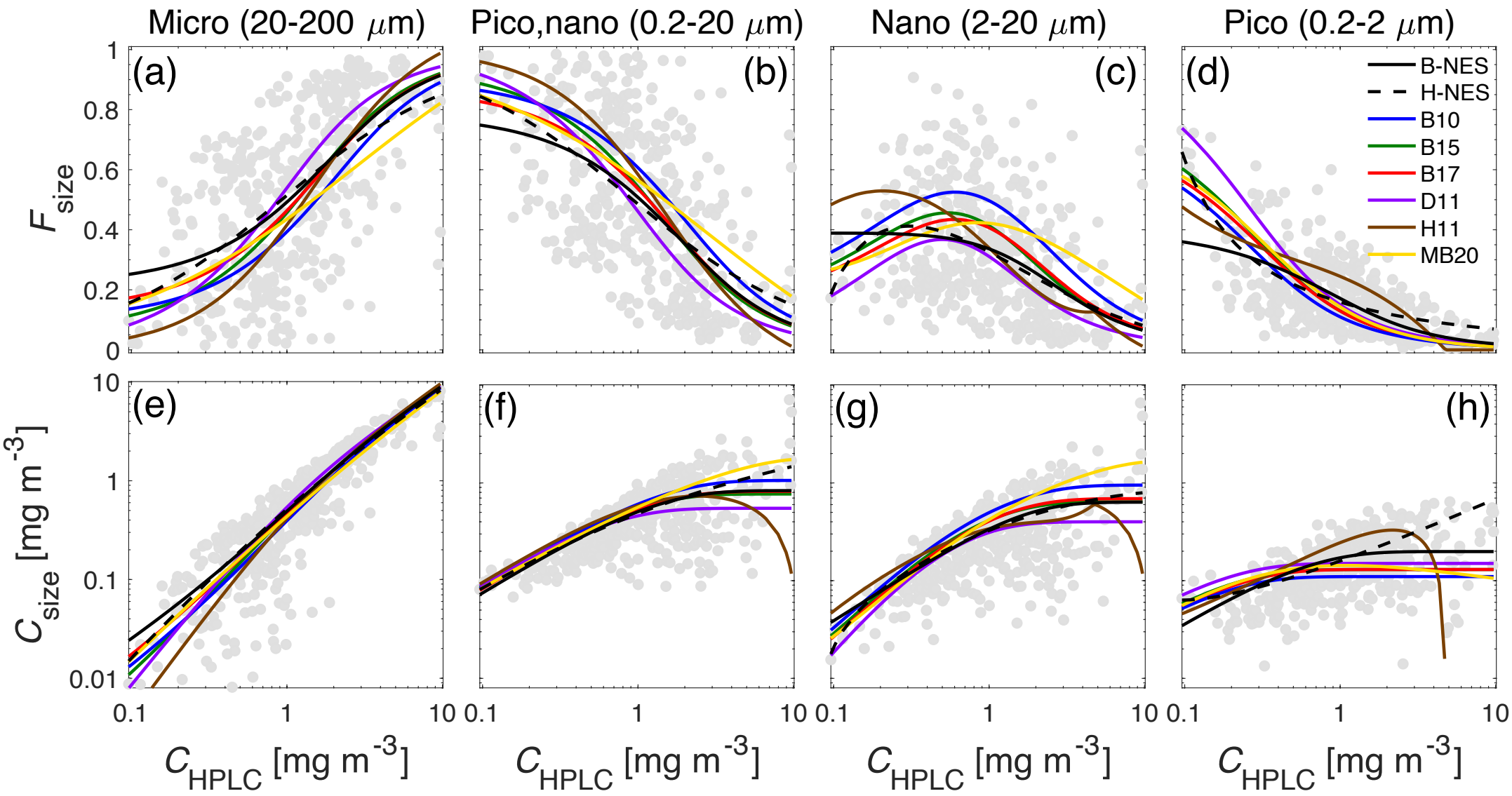

Modification of B10 model with SST

- Brewin et al. (2017) and Moore and Brown (2020) showed that incorporating *SST* into existing abundance-based model frameworks can improve performance

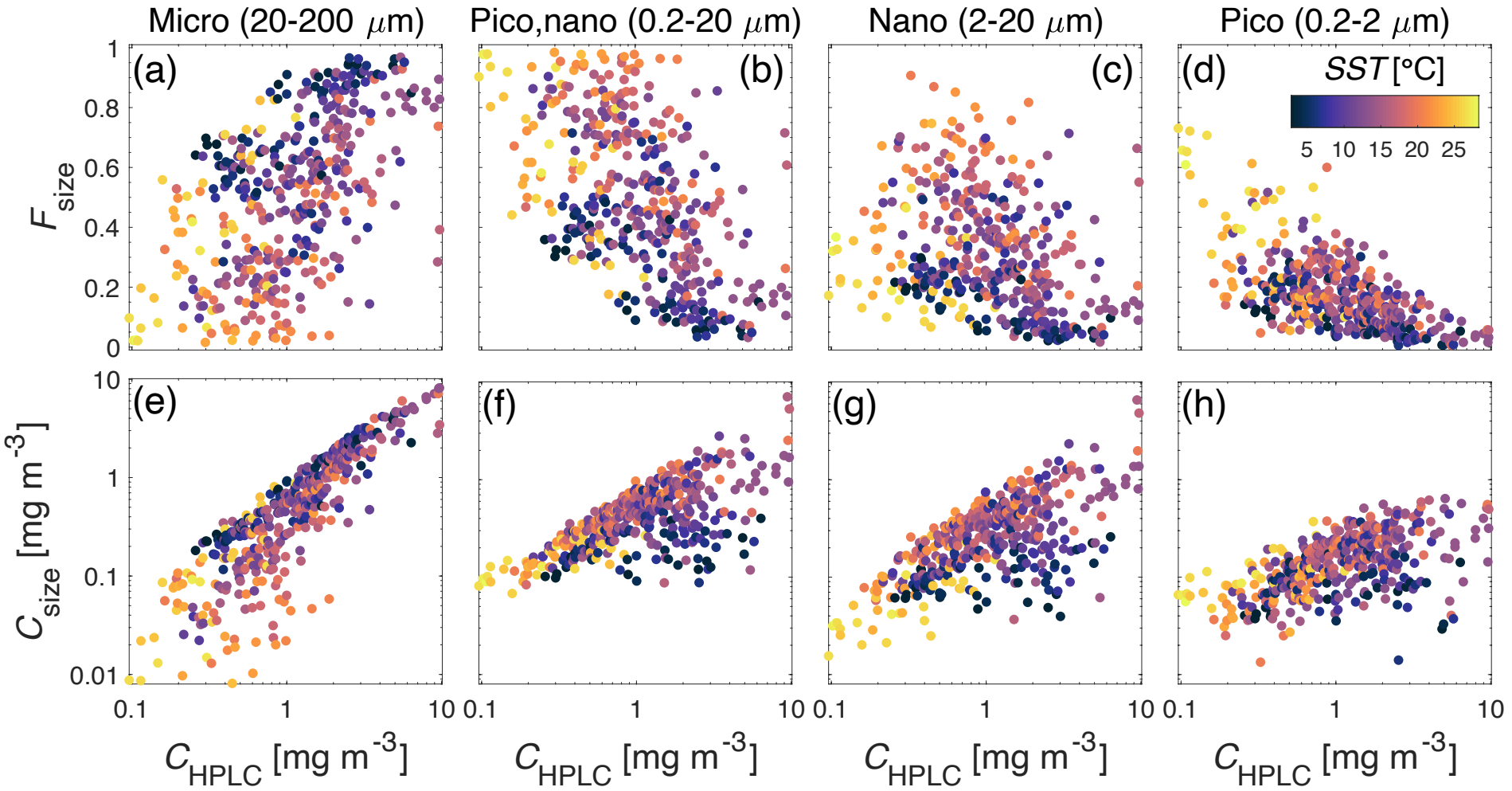

Modification of B10 model with SST

Following a similar methodology to Brewin et al. (2017) and Moore and Brown (2020)

Running fit of the model from low to high *SST* using a bin size of 125 samples:

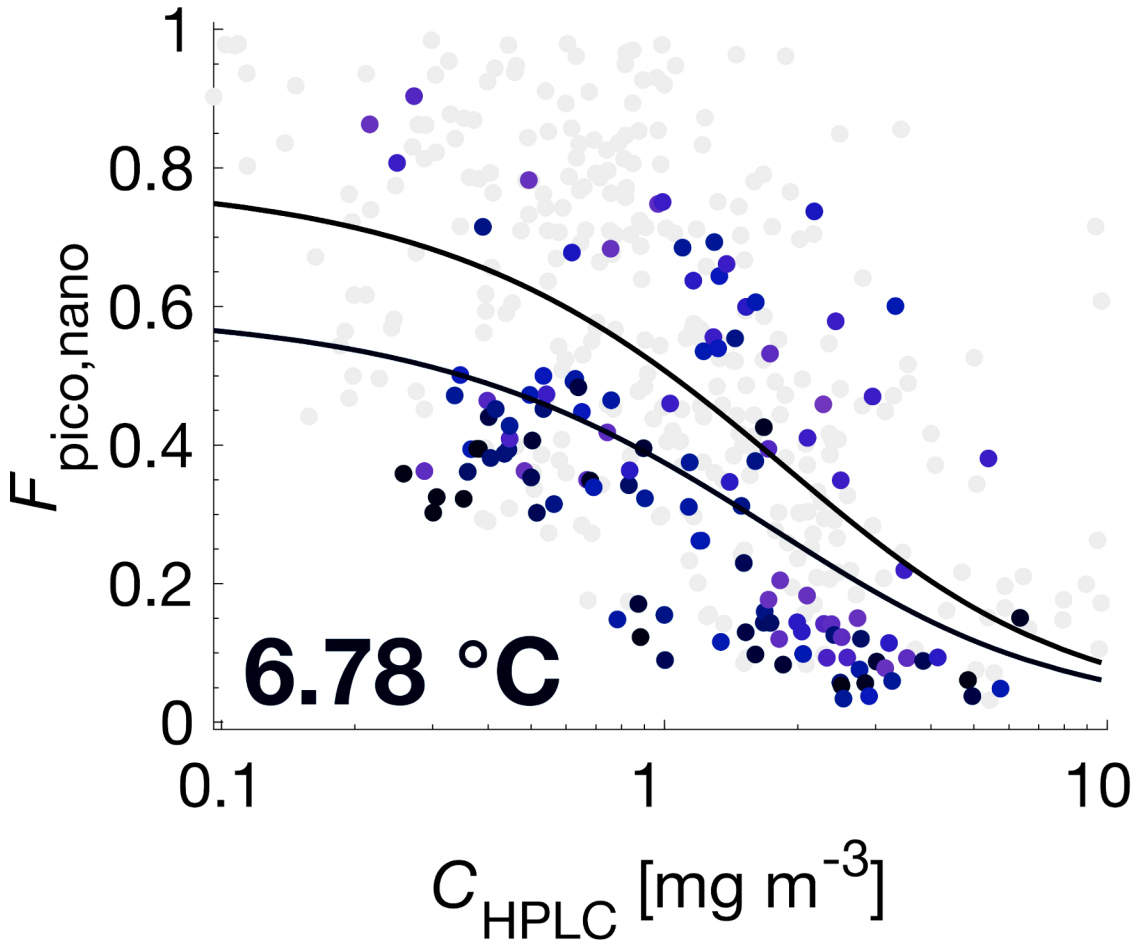

Derived model parameters as a function of the average *SST* of each bin:

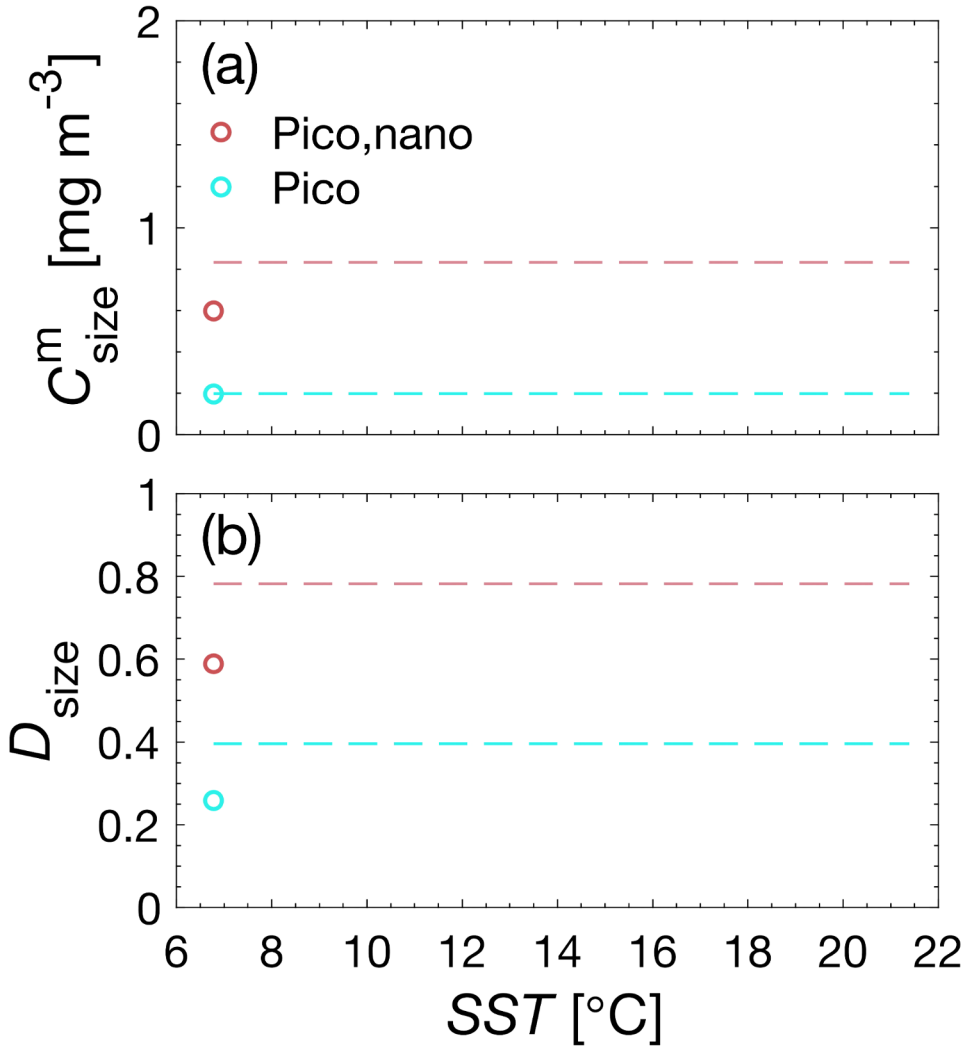

Modification of B10 model with SST

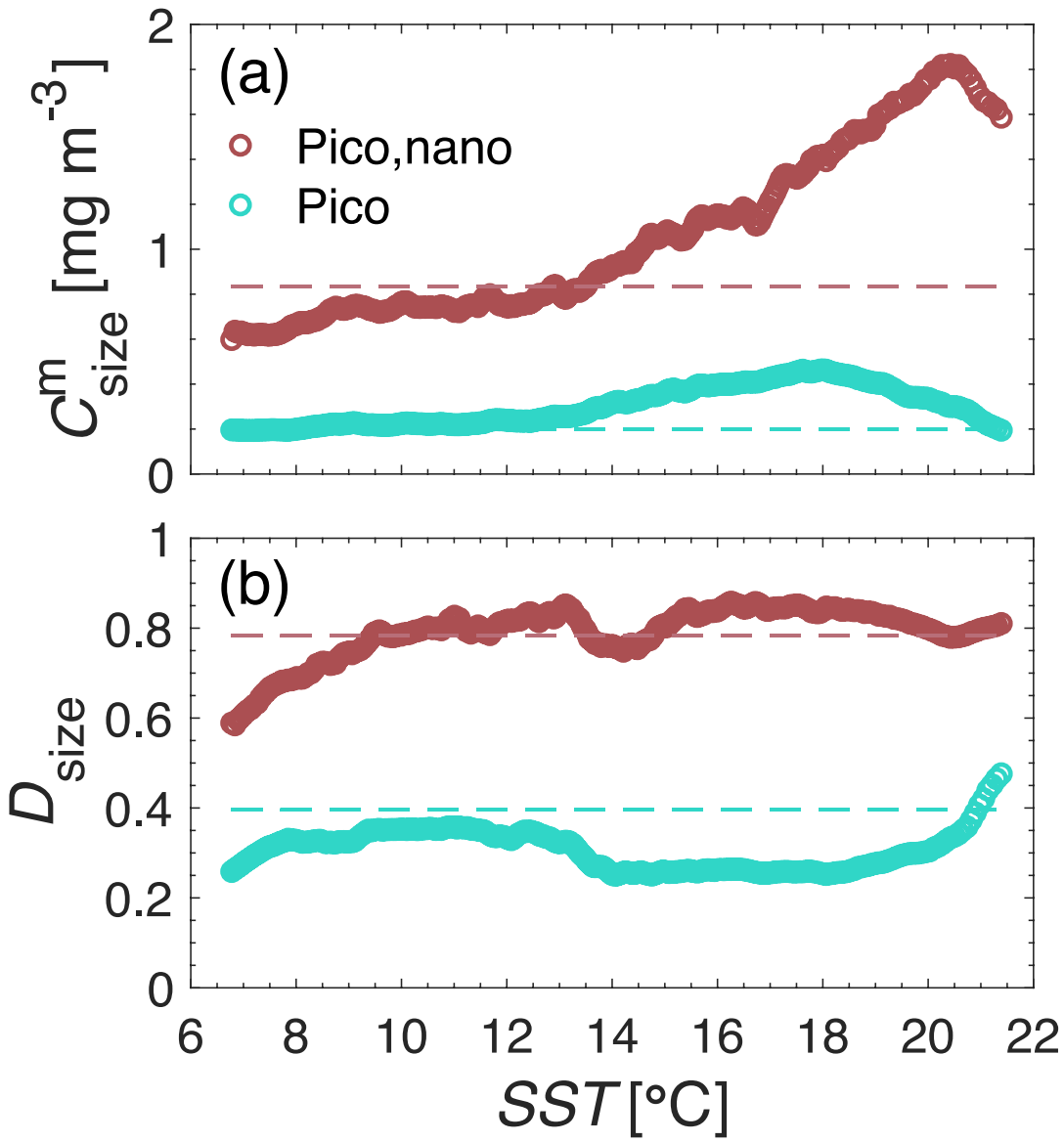

- Created a **look-up table (LUT)** for the derived model parameters indexed by *SST*
- Application of the LUT enables a dynamic set of model parameters based on observed *SST*

Regional SST-dependent B10 model (B-NES-SST)

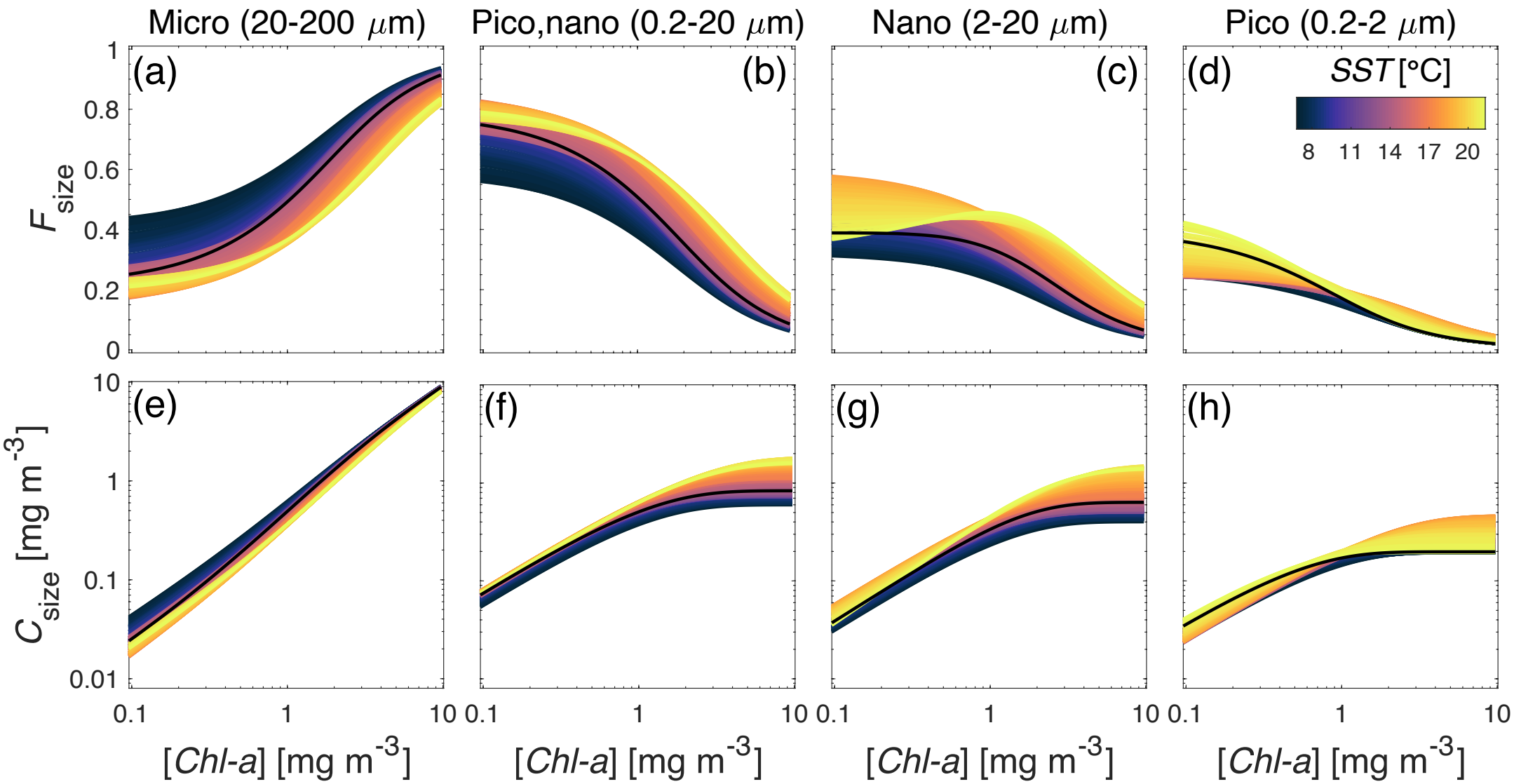

Comparison of SST-dependent models

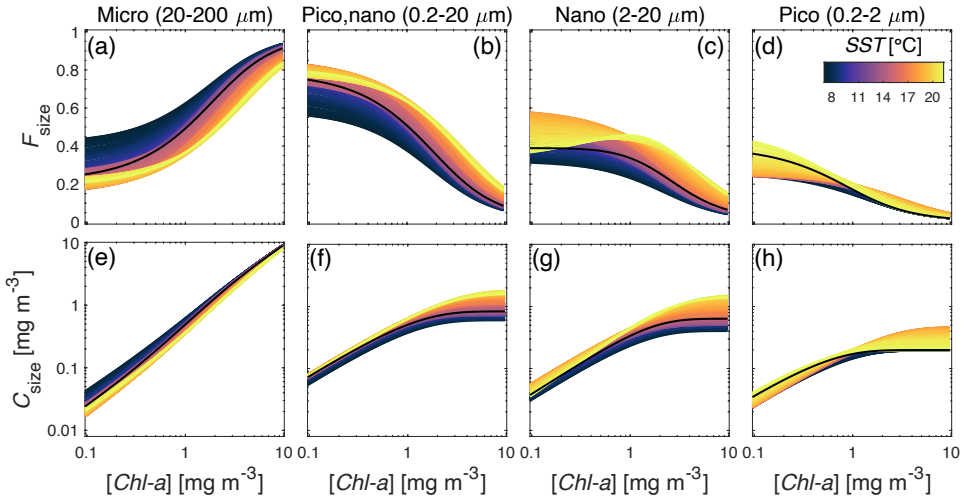

Compared with two other SST-dependent abundance-based models:

Brewin et al. (2017) [B17-*SST*]

Moore and Brown (2020) [MB20-*SST*]

Parameter	*Model*	*in situ validation set (N = 368)*			
		MAE	*% change with SST*	*r*	*% change with SST*
F_{micro} (C_{micro})	B-NES-*SST*	0.17 (0.24)	-11 (-4)	0.58 (0.87)	+32 (+2)
	B17-*SST*	0.20 (0.25)	+5 (0)	0.44 (0.85)	0 (0)
	MB20-*SST*	0.19 (0.24)	-5 (-4)	0.49 (0.86)	+9 (+1)
$F_{pico,nano}$ ($C_{pico,nano}$)	B-NES-*SST*	0.17 (0.18)	-11 (-10)	0.58 (0.77)	+32 (+6)
	B17-*SST*	0.20 (0.20)	+5 (0)	0.44 (0.72)	0 (+1)
	MB20-*SST*	0.19 (0.19)	-5 (-5)	0.49 (0.73)	+9 (0)
F_{nano} (C_{nano})	B-NES-*SST*	0.15 (0.26)	-12 (-7)	0.39 (0.79)	+225 (+6)
	B17-*SST*	0.16 (0.27)	-6 (-4)	0.29 (0.75)	+45 (+1)
	MB20-*SST*	0.16 (0.27)	-11 (-7)	0.18 (0.72)	0 (-3)
F_{pico} (C_{pico})	B-NES-*SST*	0.09 (0.20)	-10 (-9)	0.73 (0.62)	+16 (+15)
	B17-*SST*	0.09 (0.23)	-10 (-4)	0.73 (0.53)	+4 (+23)
	MB20-*SST*	0.10 (0.22)	0 (-8)	0.72 (0.52)	+3 (+37)

Comparison of SST-dependent models

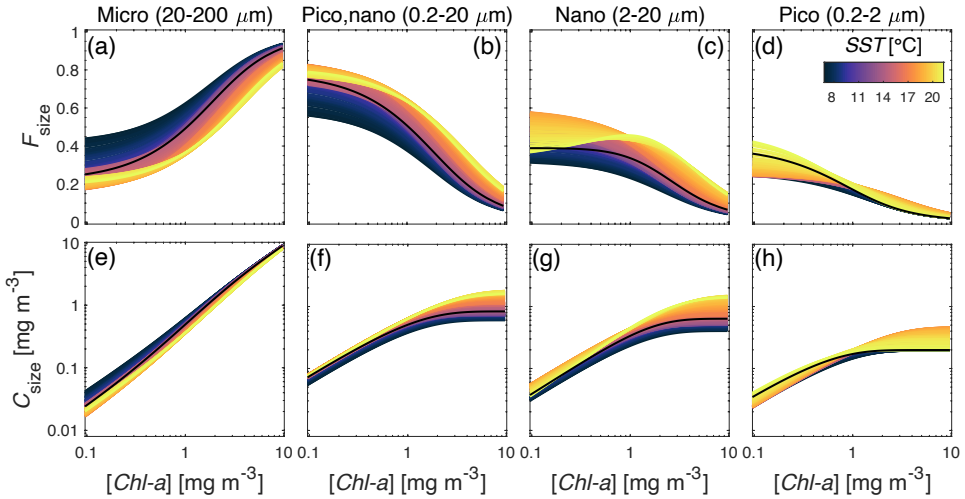

- **Addition of *SST* consistently decreased error and increased correlation coefficient for all size classes**

Parameter	Model	*in situ validation set (N = 368)*			
		MAE	*% change with SST*	*r*	*% change with SST*
F_{micro} (C_{micro})	B-NES-*SST*	0.17 (0.24)	-11 (-4)	0.58 (0.87)	+32 (+2)
	B17-*SST*	0.20 (0.25)	+5 (0)	0.44 (0.85)	0 (0)
	MB20-*SST*	0.19 (0.24)	-5 (-4)	0.49 (0.86)	+9 (+1)
$F_{pico,nano}$ ($C_{pico,nano}$)	B-NES-*SST*	0.17 (0.18)	-11 (-10)	0.58 (0.77)	+32 (+6)
	B17-*SST*	0.20 (0.20)	+5 (0)	0.44 (0.72)	0 (+1)
	MB20-*SST*	0.19 (0.19)	-5 (-5)	0.49 (0.73)	+9 (0)
F_{nano} (C_{nano})	B-NES-*SST*	0.15 (0.26)	-12 (-7)	0.39 (0.79)	+225 (+6)
	B17-*SST*	0.16 (0.27)	-6 (-4)	0.29 (0.75)	+45 (+1)
	MB20-*SST*	0.16 (0.27)	-11 (-7)	0.18 (0.72)	0 (-3)
F_{pico} (C_{pico})	B-NES-*SST*	0.09 (0.20)	-10 (-9)	0.73 (0.62)	+16 (+15)
	B17-*SST*	0.09 (0.23)	-10 (-4)	0.73 (0.53)	+4 (+23)
	MB20-*SST*	0.10 (0.22)	0 (-8)	0.72 (0.52)	+3 (+37)

Compared with two other SST-dependent abundance-based models:

Brewin et al. (2017) [B17-*SST*]

Moore and Brown (2020) [MB20-*SST*]

Comparison of SST-dependent models

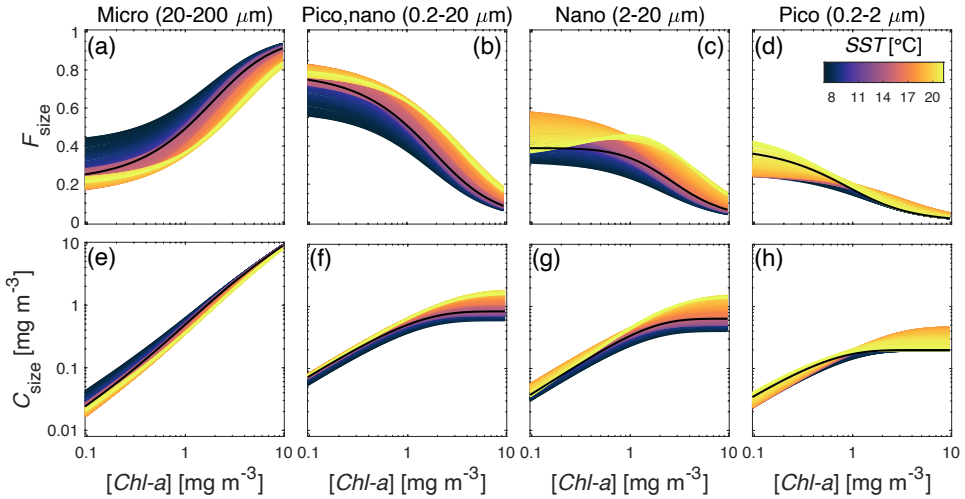

Compared with two other SST-dependent abundance-based models:

Brewin et al. (2017) [B17-*SST*]

Moore and Brown (2020) [MB20-*SST*]

- **B-NES-*SST* model consistently out-performed the other two *SST*-dependent models**

Parameter	*Model*	*in situ validation set (N = 368)*			
		MAE	*% change with SST*	*r*	*% change with SST*
F_{micro} (C_{micro})	B-NES-*SST*	0.17 (0.24)	-11 (-4)	0.58 (0.87)	+32 (+2)
	B17-*SST*	0.20 (0.25)	+5 (0)	0.44 (0.85)	0 (0)
	MB20-*SST*	0.19 (0.24)	-5 (-4)	0.49 (0.86)	+9 (+1)
$F_{pico,nano}$ ($C_{pico,nano}$)	B-NES-*SST*	0.17 (0.18)	-11 (-10)	0.58 (0.77)	+32 (+6)
	B17-*SST*	0.20 (0.20)	+5 (0)	0.44 (0.72)	0 (+1)
	MB20-*SST*	0.19 (0.19)	-5 (-5)	0.49 (0.73)	+9 (0)
F_{nano} (C_{nano})	B-NES-*SST*	0.15 (0.26)	-12 (-7)	0.39 (0.79)	+225 (+6)
	B17-*SST*	0.16 (0.27)	-6 (-4)	0.29 (0.75)	+45 (+1)
	MB20-*SST*	0.16 (0.27)	-11 (-7)	0.18 (0.72)	0 (-3)
F_{pico} (C_{pico})	B-NES-*SST*	0.09 (0.20)	-10 (-9)	0.73 (0.62)	+16 (+15)
	B17-*SST*	0.09 (0.23)	-10 (-4)	0.73 (0.53)	+4 (+23)
	MB20-*SST*	0.10 (0.22)	0 (-8)	0.72 (0.52)	+3 (+37)

Validation of satellite total [Chl-a]

- **Compared the standard OC-CCI [*Chl-a*] algorithm with the regional algorithm of Pan et al. (2010)**

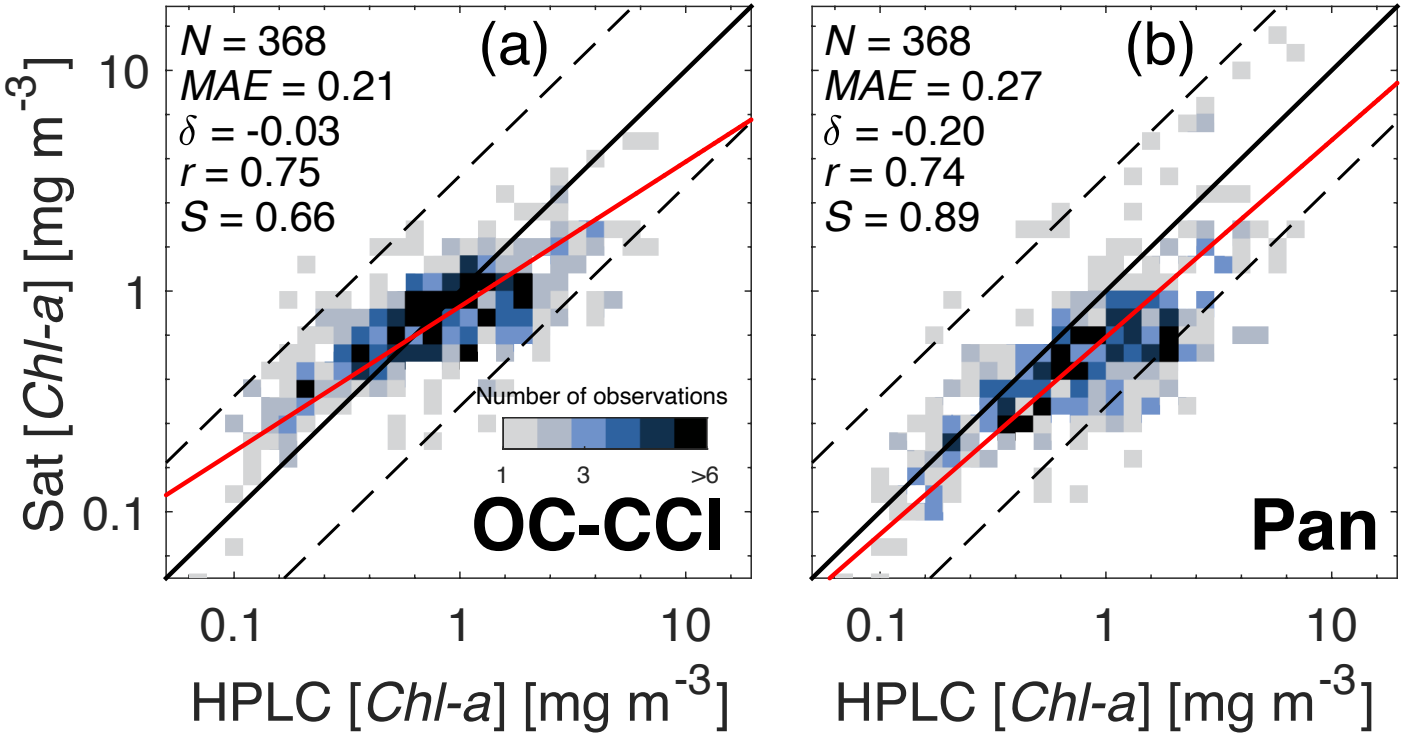

- **OC-CCI [*Chl-a*] algorithm showed similar performance in the NES to the global validation (*N* = 18,482)**

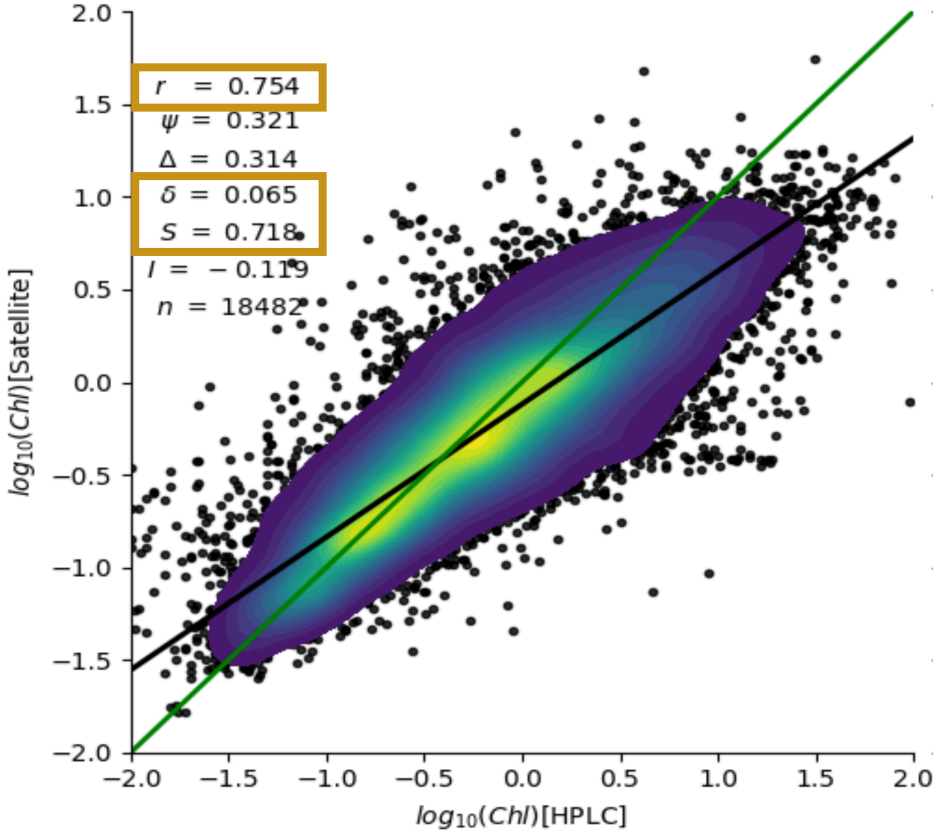

https://docs.pml.space/share/s/dPL4zFuaT_eFa-mTLU9nQA

Validation of satellite size-specific [Chl-a]

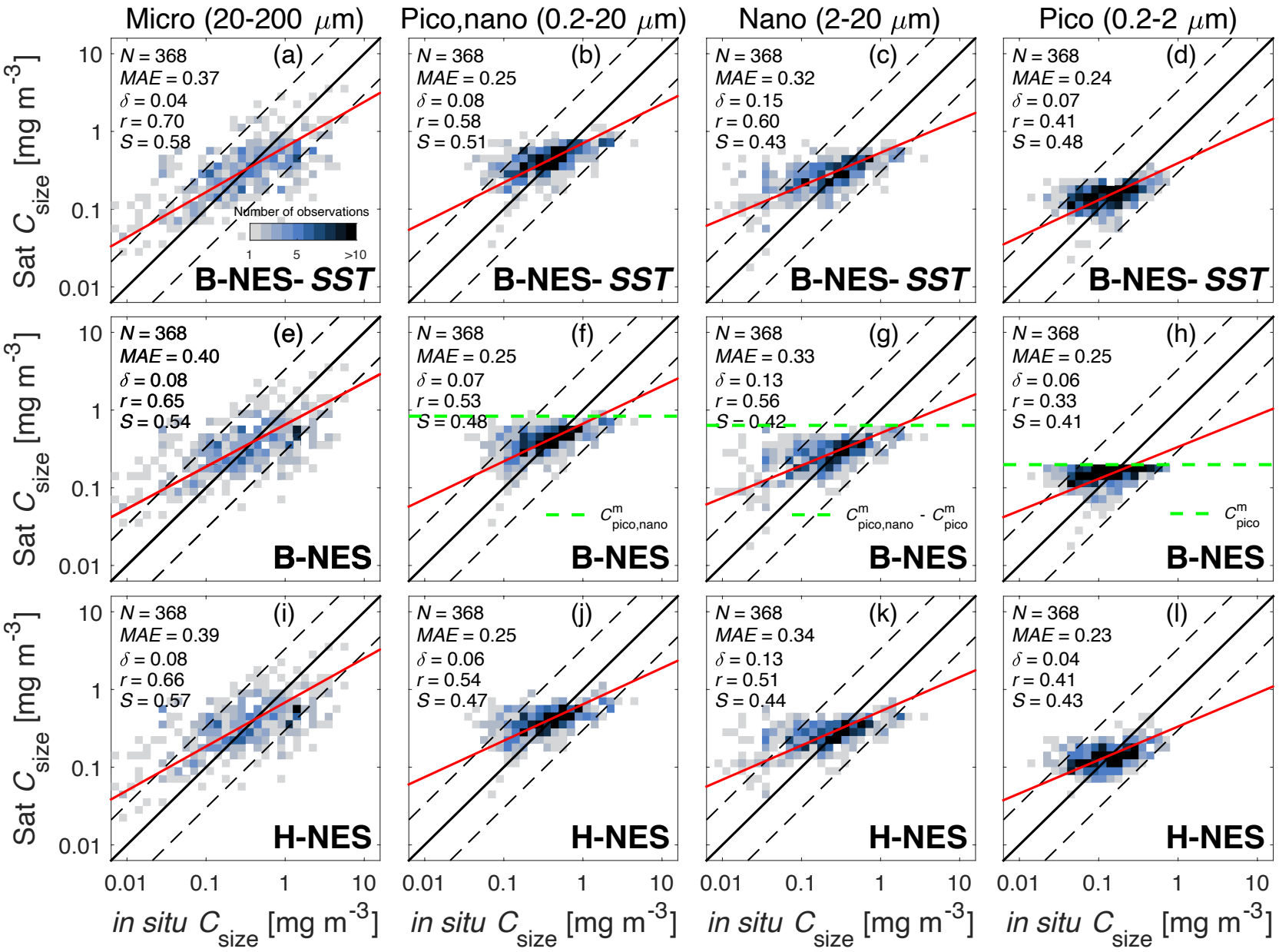

Validation of satellite size-specific [Chl-a]

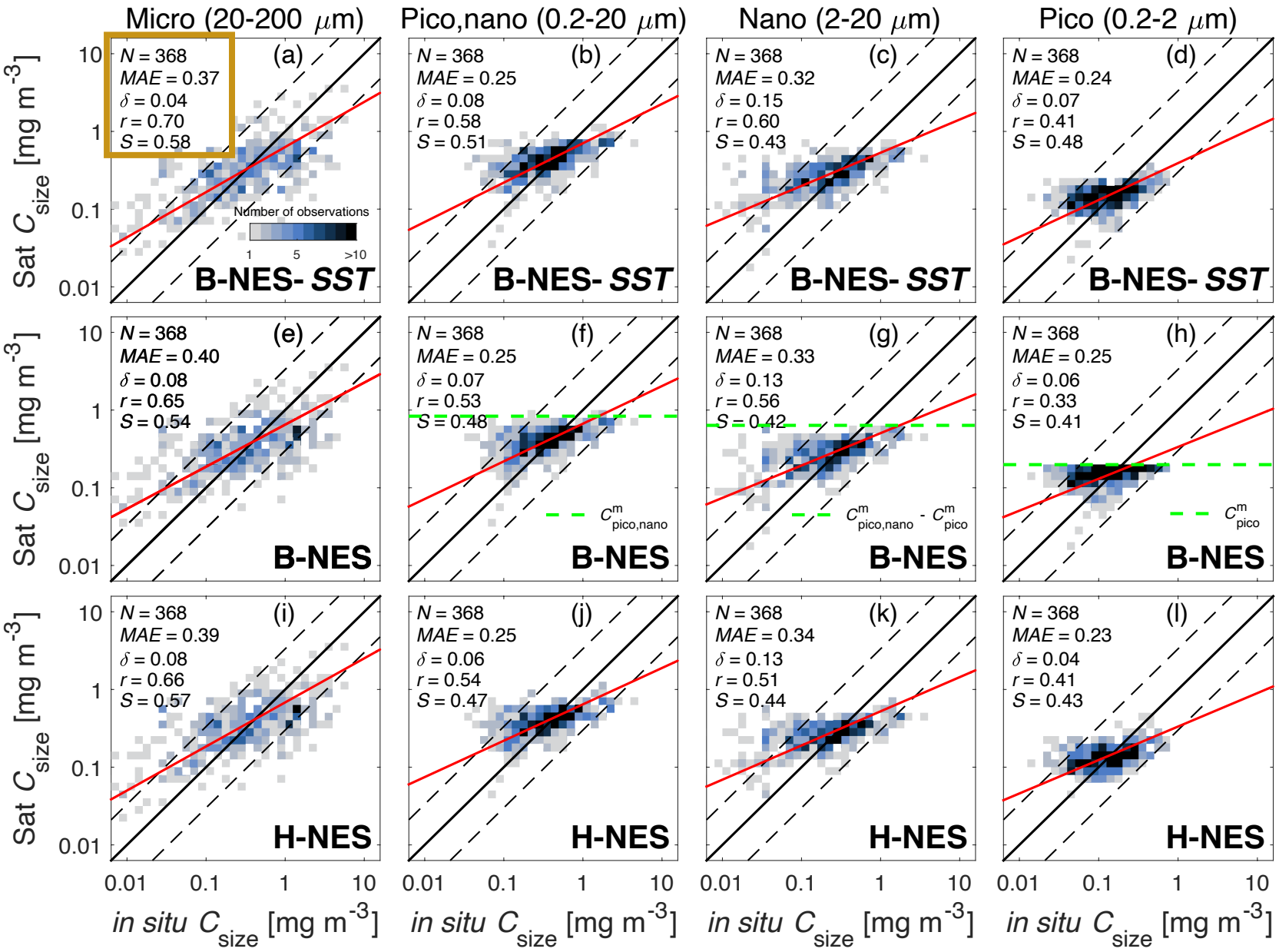

- **B-NES-*SST* model showed largest improvement for C_{micro}**

Validation of satellite size-specific [Chl-a]

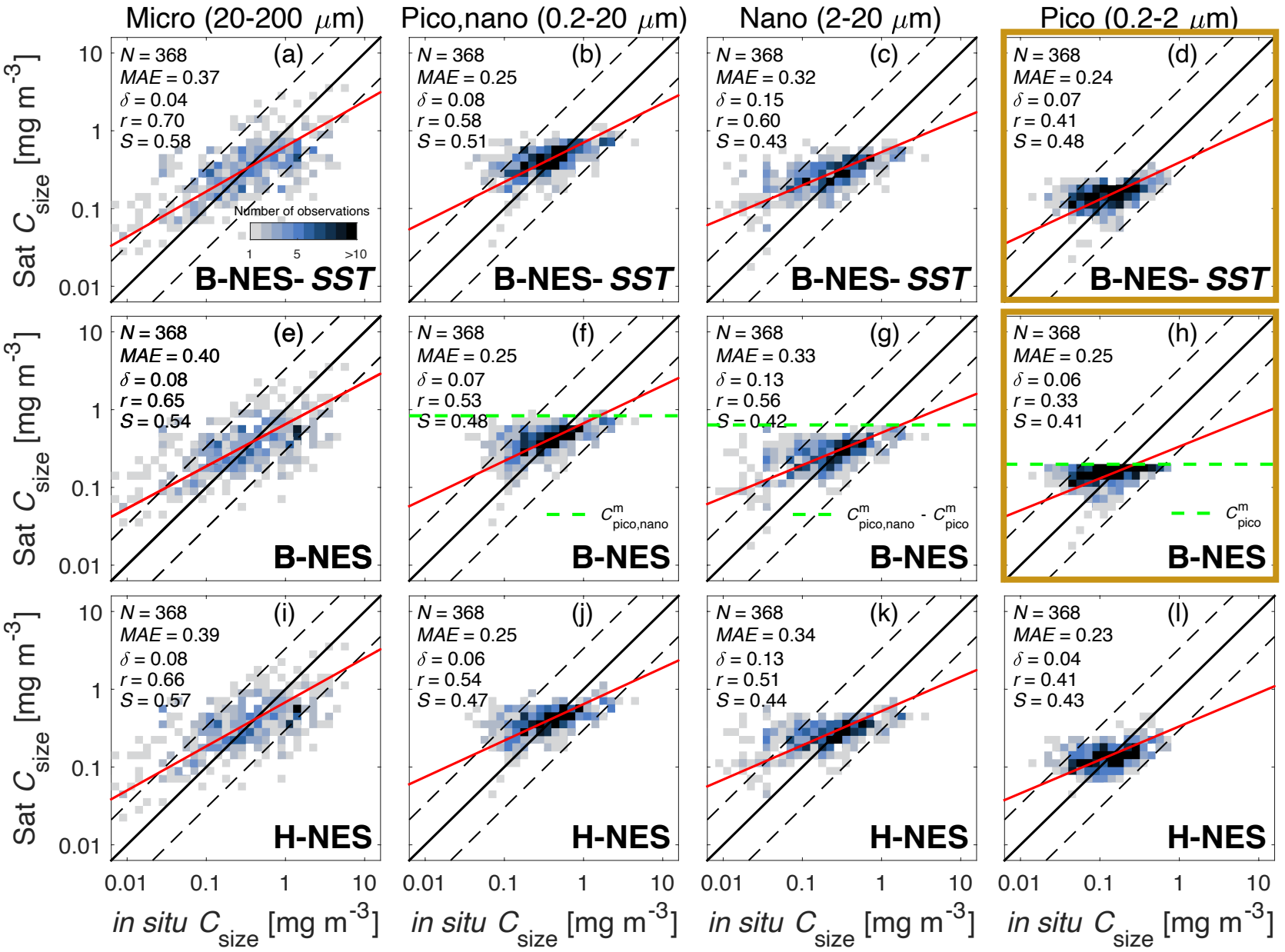

- **B-NES-*SST* model showed largest improvement for C_{micro}**
- **B-NES-*SST* model less constrained by static maximums than B-NES model** *consistent with Brewin et al. (2017)*

Absorption-based algorithms

Estimate the fractional contribution of PSCs based on changes in phytoplankton absorption [$a_{ph}(\lambda)$]

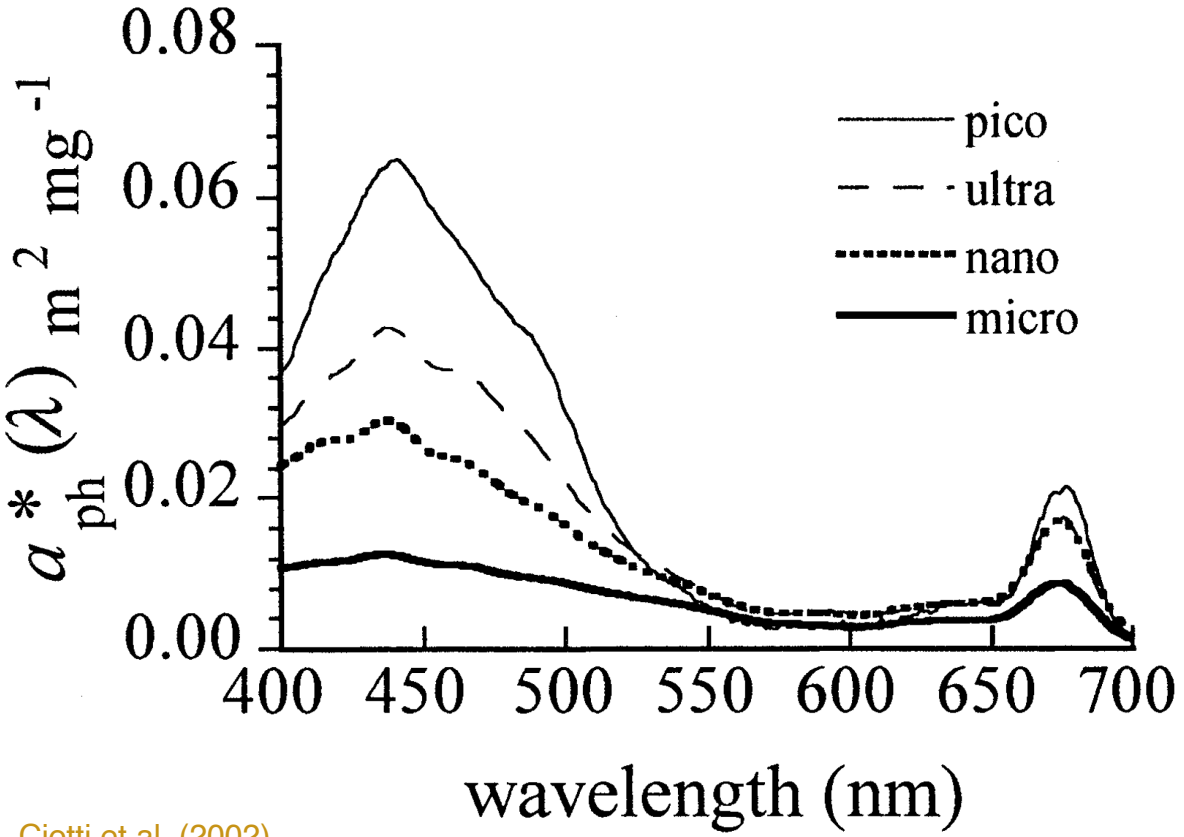

Ciotti et al. (2002)

$a_{ph}^*(\lambda)$ = chlorophyll-normalized phytoplankton absorption

- Smaller cells **more efficient** light absorbers
- Larger cells **less efficient** light absorbers

Ciotti et al. (2002)

$$a^*_{ph}(\lambda) = \left[F_{pico} * \bar{a}^*_{pico}(\lambda)\right] + \left[\left(1 - F_{pico}\right) * \bar{a}^*_{micro}(\lambda)\right]$$

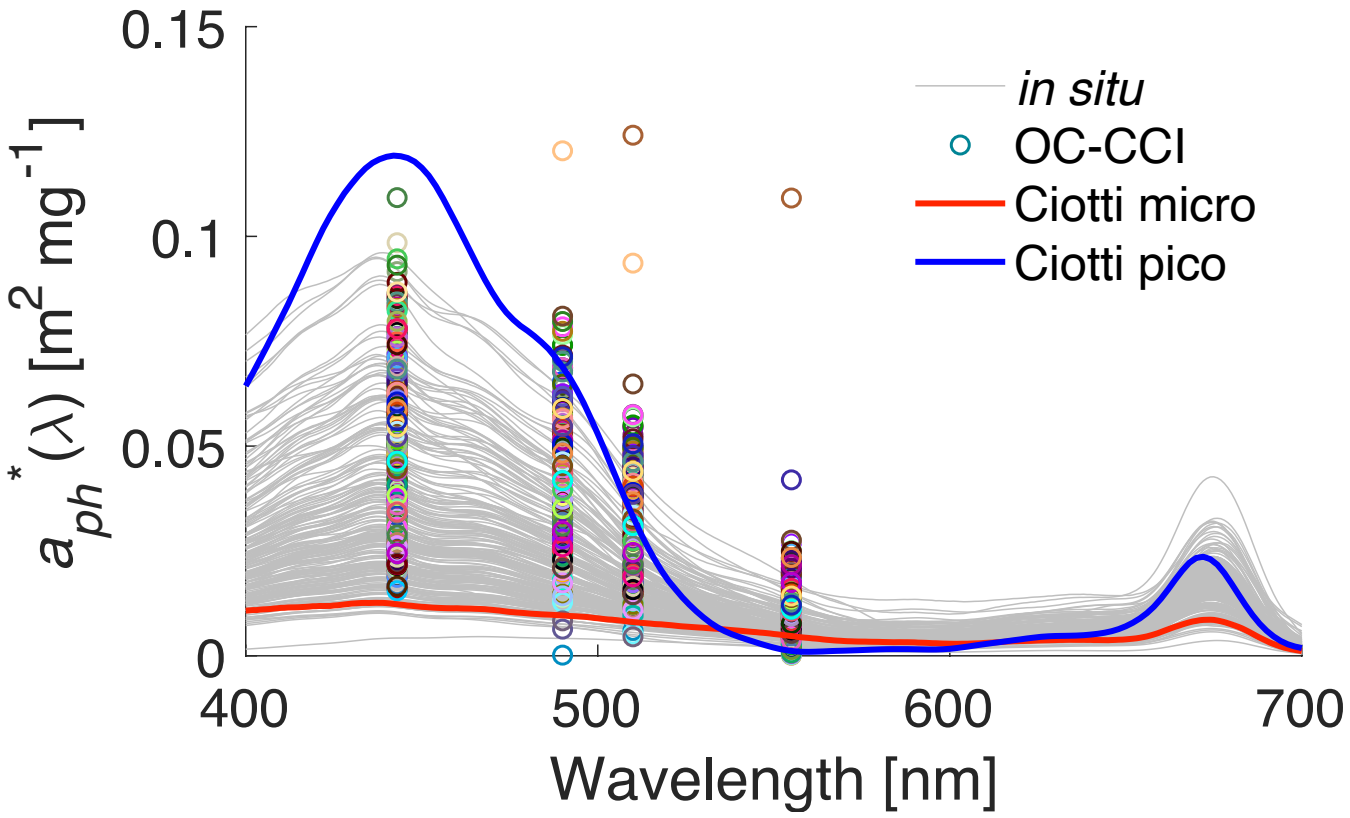

- Satellite $a_{ph}^*(\lambda)$ calculated as satellite $a_{ph}(\lambda)$/satellite [*Chl-a*]
- F_{pico} computed by linear least squares optimization using published basis spectra at four wavelengths (443, 490, 510, 555 nm)
- $F_{micro,nano} = 1 - F_{pico}$

Mouw and Yoder (2010)

- Employs an optical LUT containing ranges of [*Chl-a*], $a_{dg}(443)$, and F_{micro} from which $R_{rs}(\lambda)$ was modeled using the radiative transfer modeling software HydroLight[1]

- Uses satellite [*Chl-a*] and $a_{dg}(443)$ as input to narrow the search space of the LUT, and the closest matching LUT $R_{rs}(\lambda)$ to the satellite $R_{rs}(\lambda)$ is found to retrieve the corresponding F_{micro}

- $F_{pico,nano} = 1 - F_{micro}$

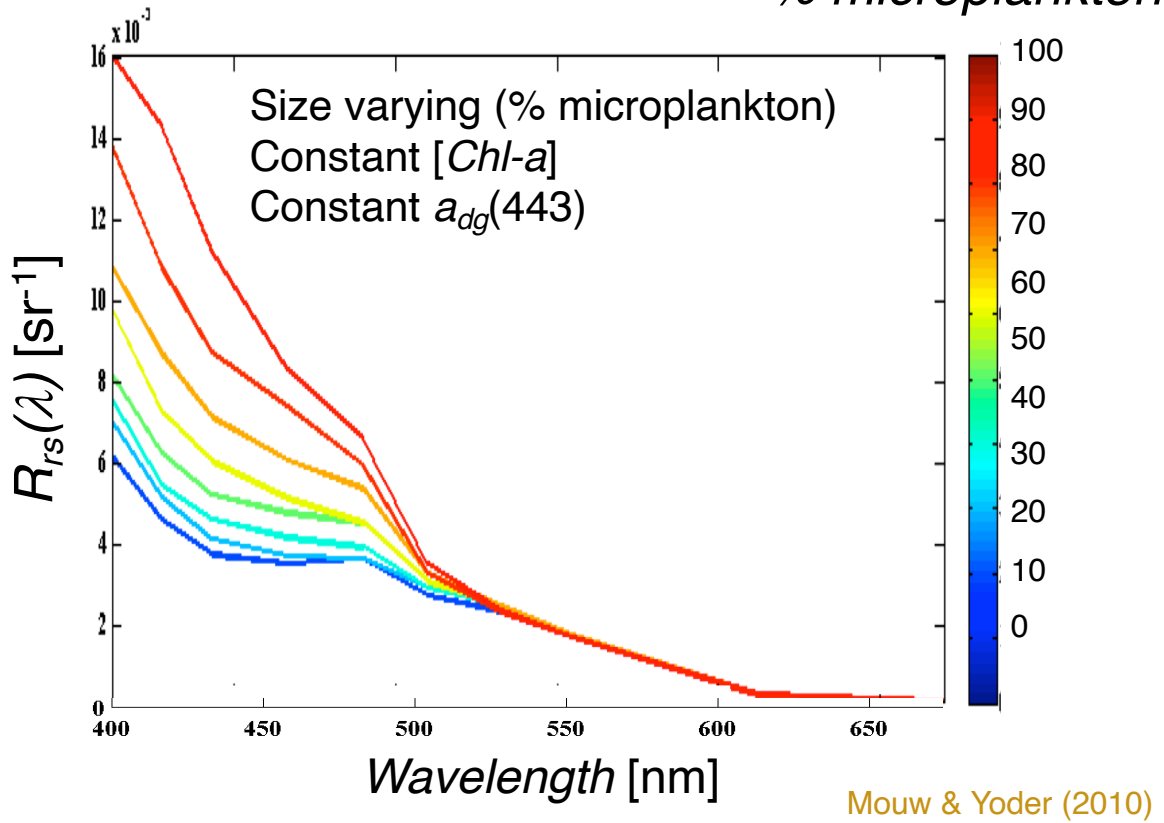

Mouw & Yoder (2010)

[1]Mobley and Sundman (2013)

Validation of satellite $a_{ph}(\lambda)$ and $a_{dg}(\lambda)$

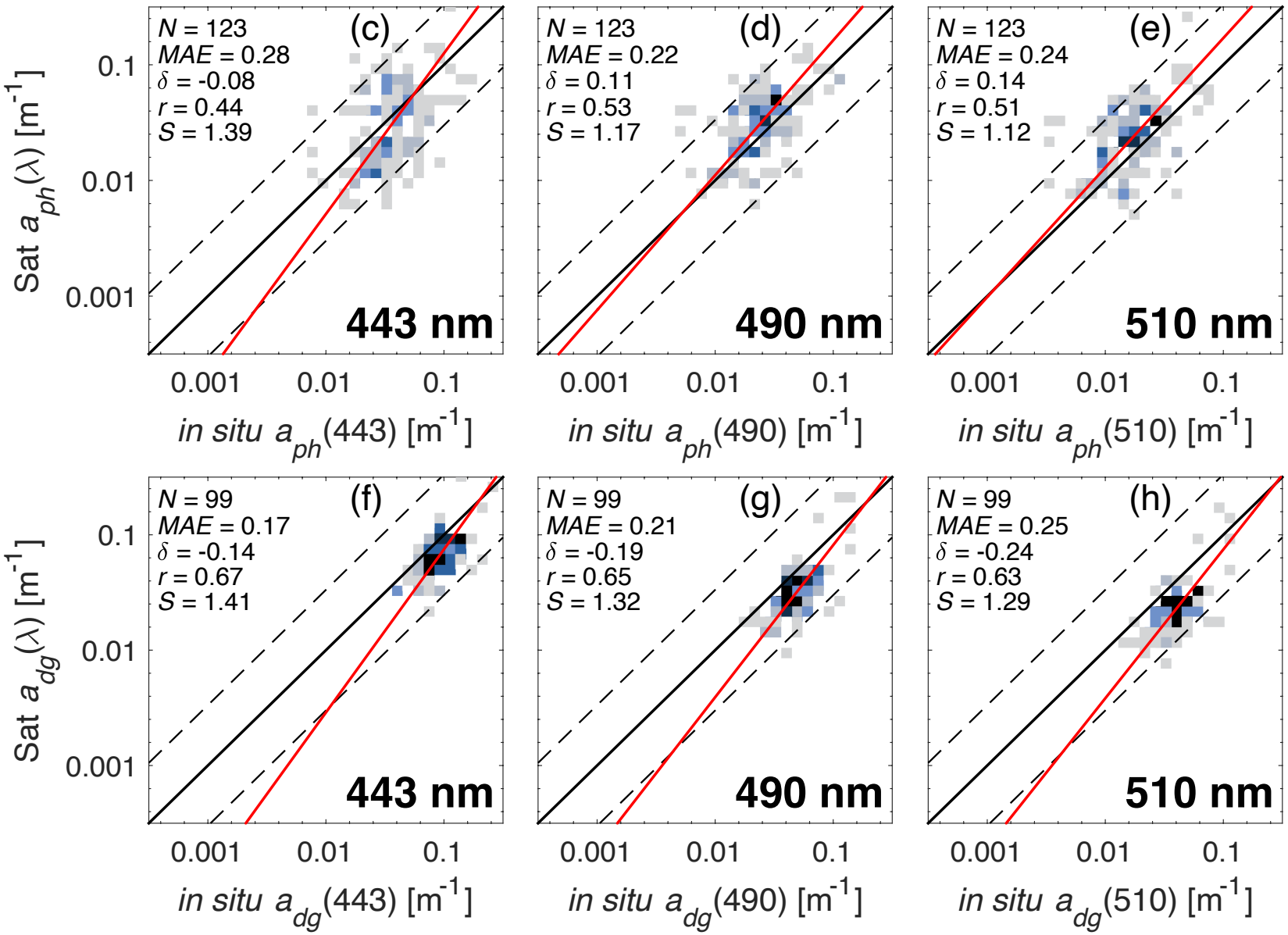

Validation of satellite size-specific [Chl-a]

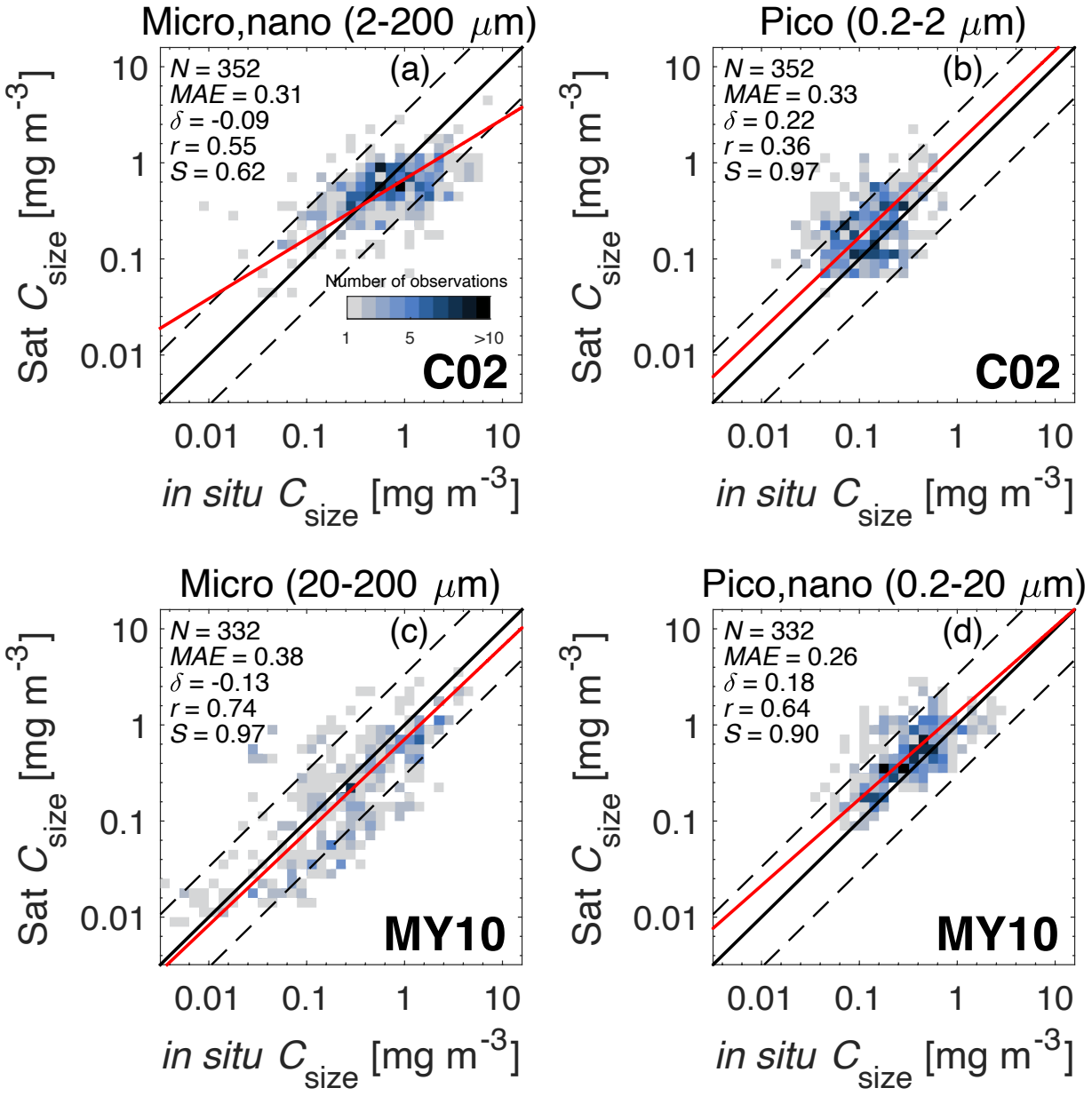

Validation of satellite size-specific [Chl-a]

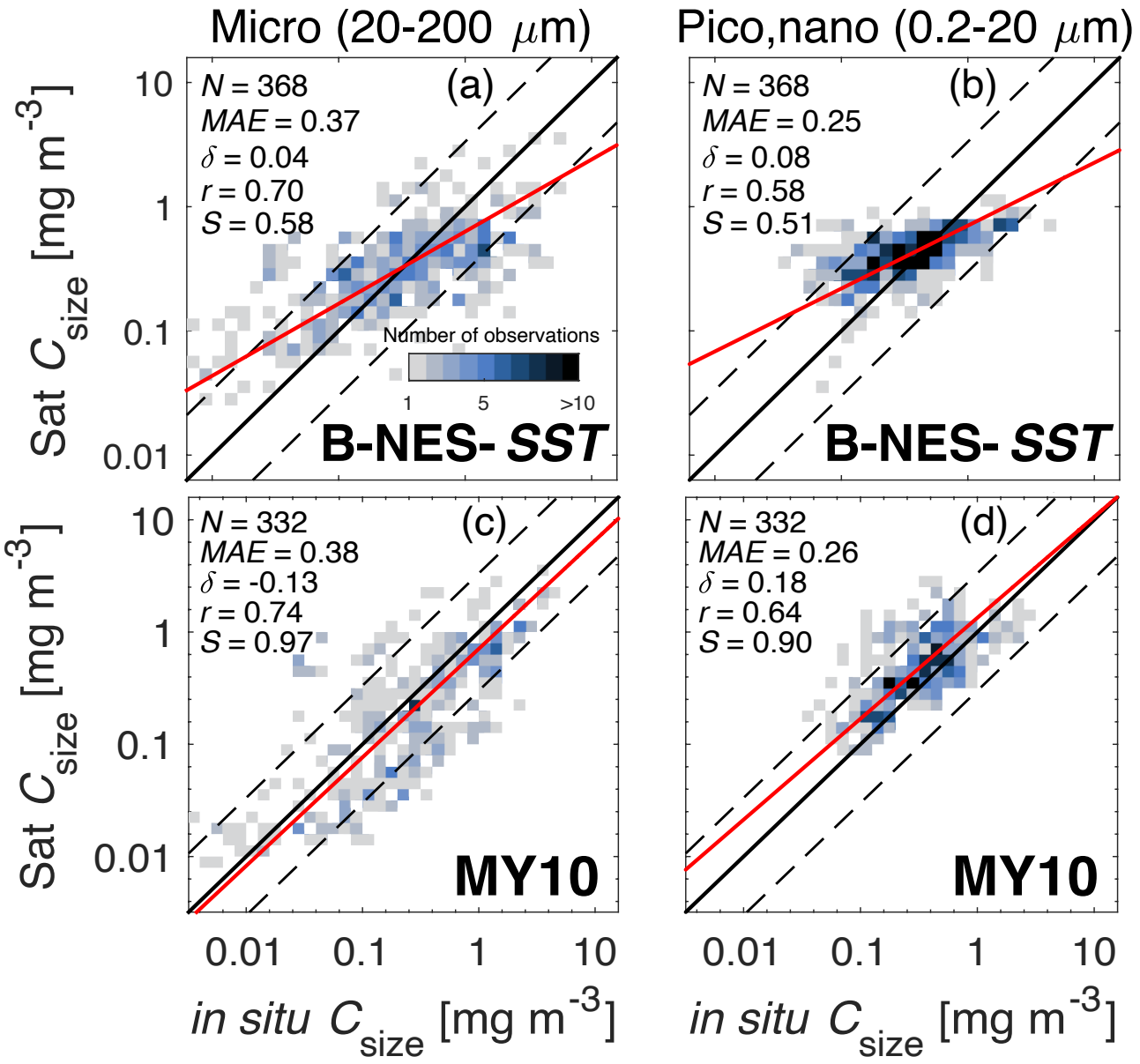

- **MY10 model performed with similar error as the B-NES-*SST* model, but with improved correlation coefficients and regression slope values**

Examples of regional imagery

Black line indicates the 400 m isobath

April 2019

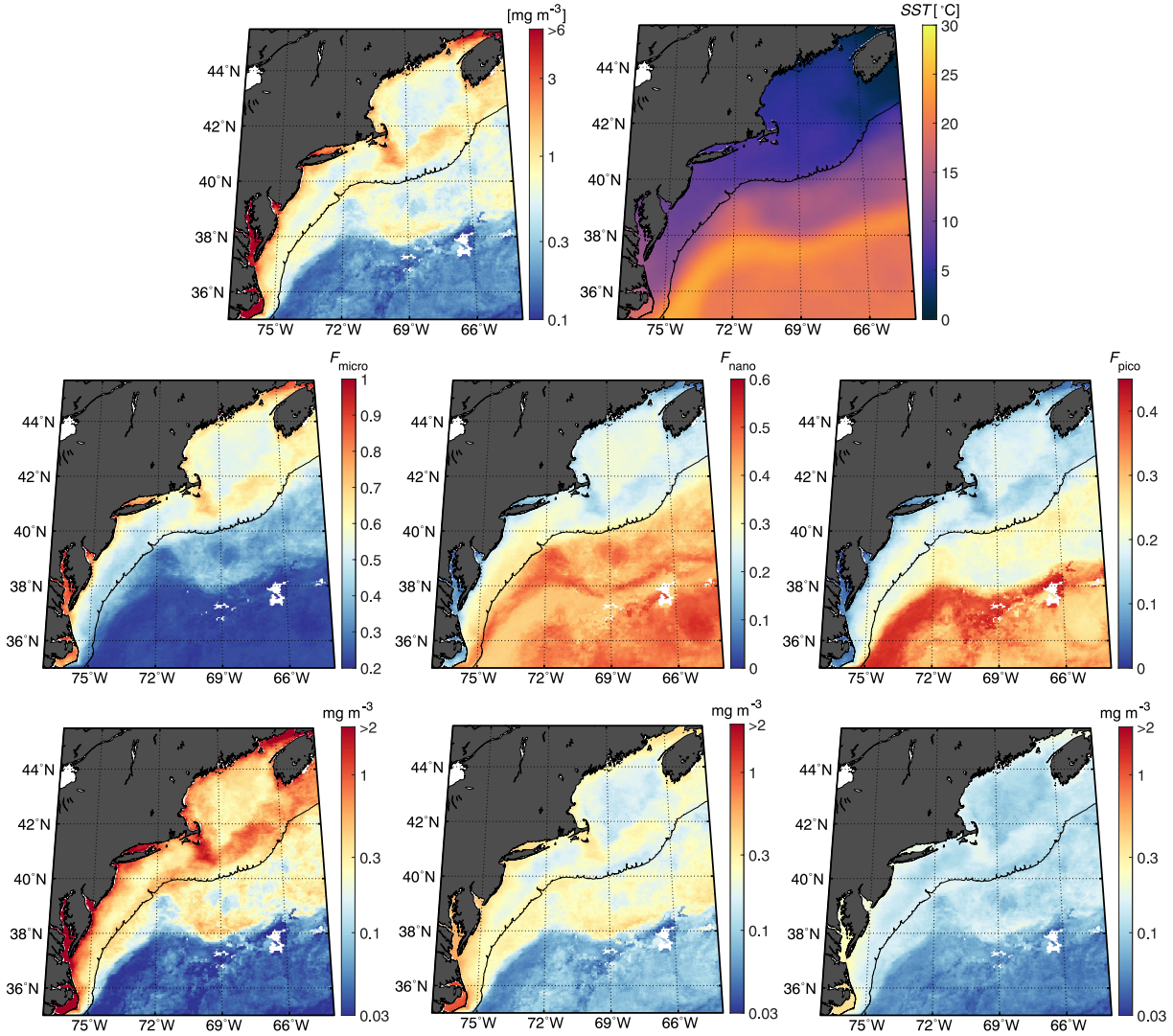

September 2019

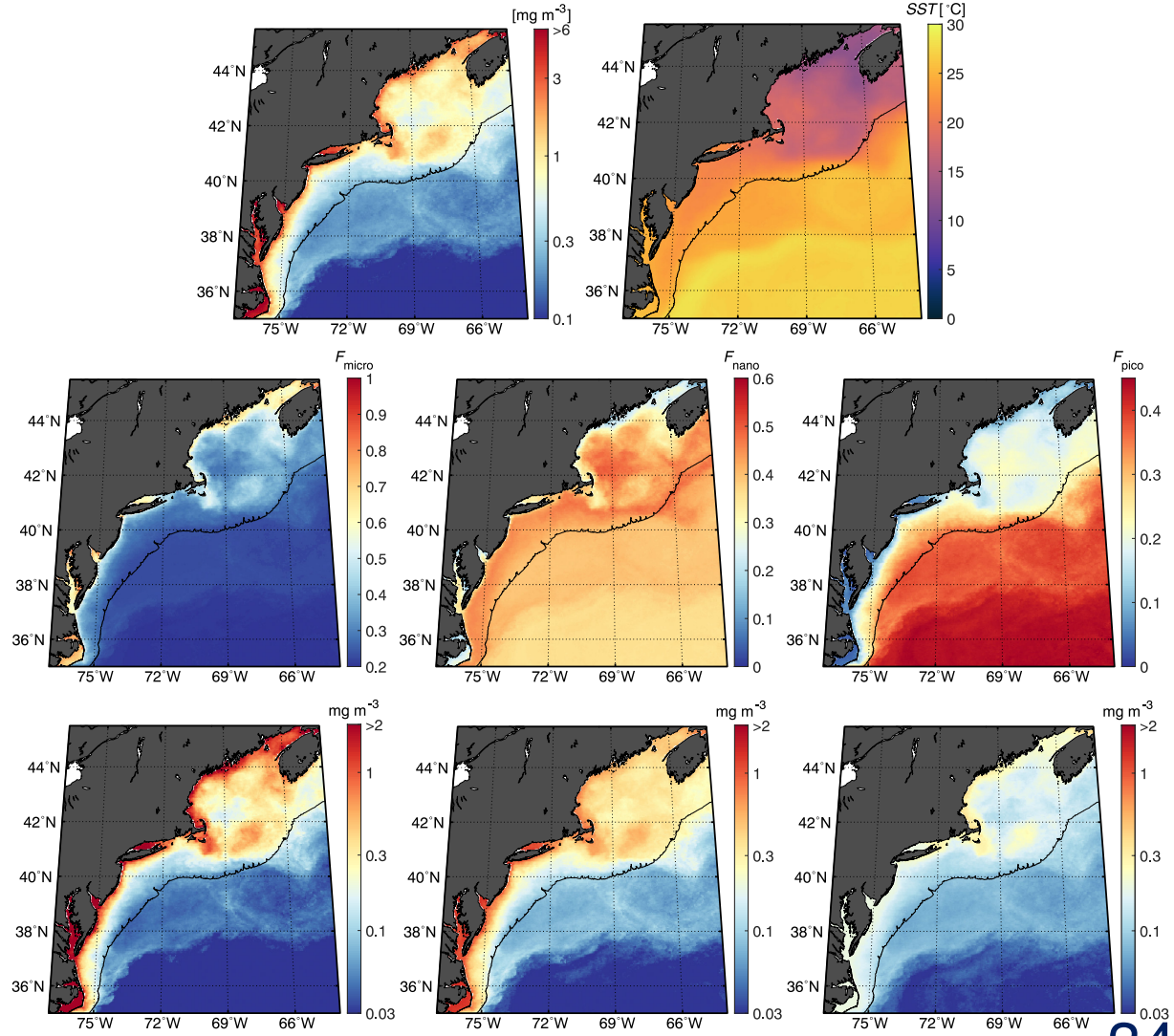

Comparison of B-NES-SST and MY10 imagery

B-NES-SST | **MY10**

April 2019

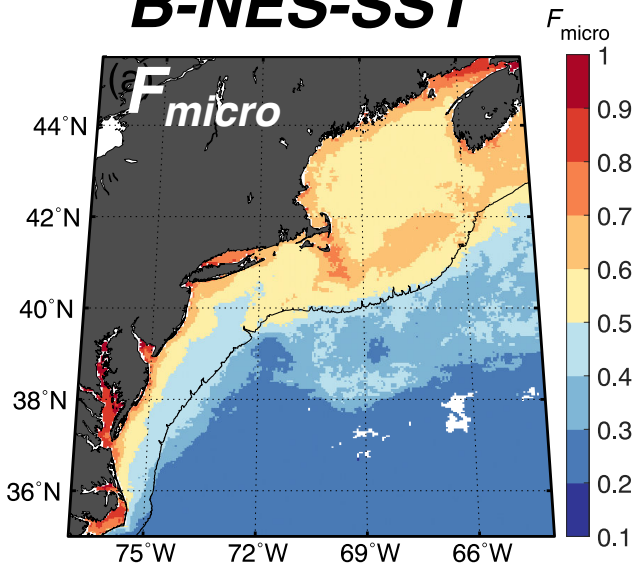

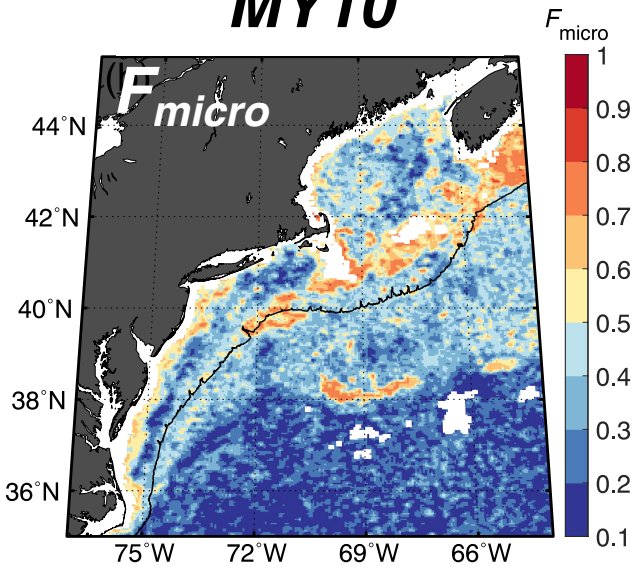

September 2019

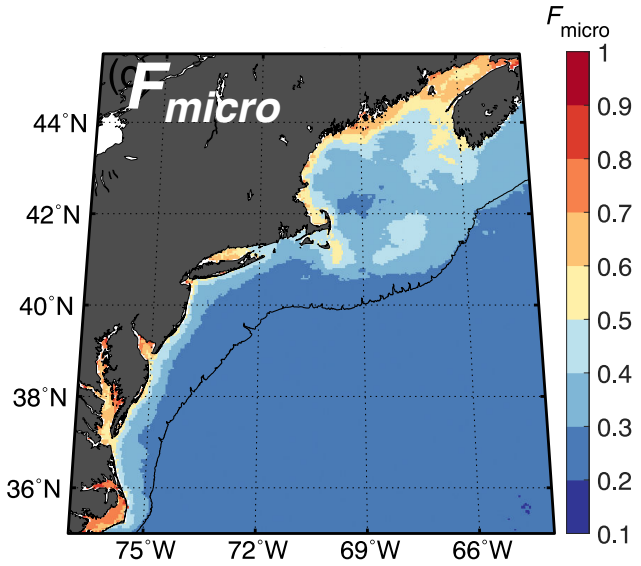

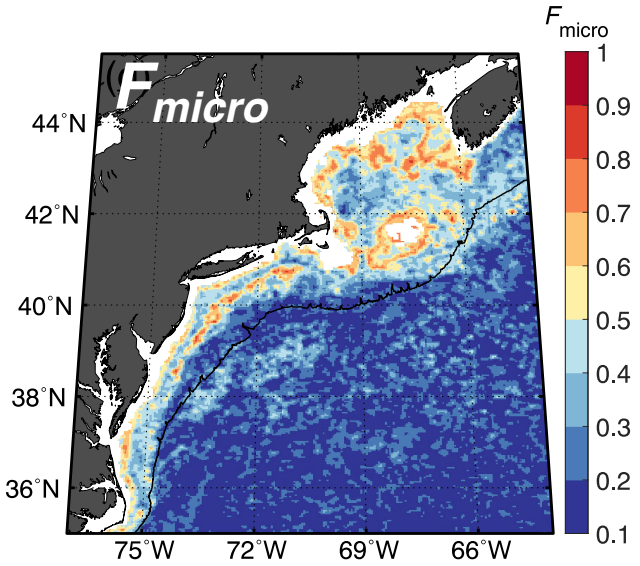

Black line indicates the 400 m isobath

Summary

- Abundance-based model re-parameterization alone did not result in significant improvement in performance in the NES compared with other models
- The incorporation of *SST* into the re-parameterization of the B10 model did improve PSC prediction accuracy
- Absorption-based models showed comparable performance to abundance-based models at estimating size-specific [*Chl-a*] in the NES

Application: The regional B-NES-*SST* model is currently being integrated into the Northeast U.S. implementation of the ATLANTIS ecosystem model and incorporated into other NOAA ecosystem-based fisheries management products

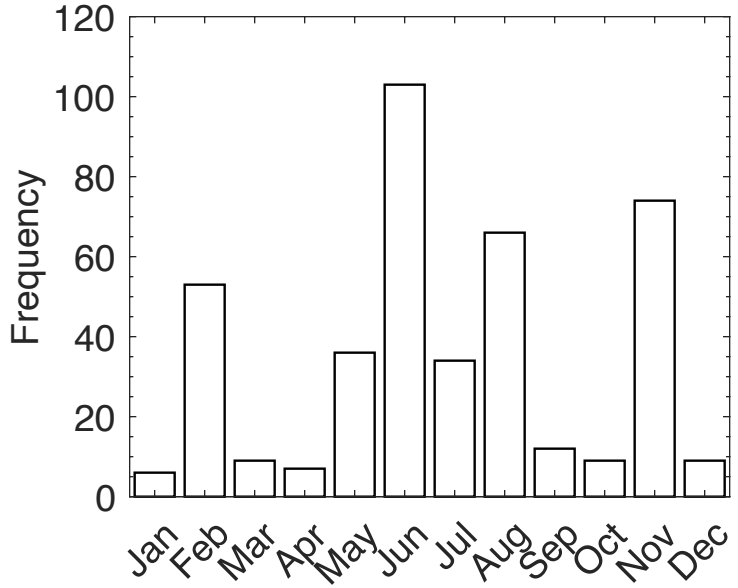

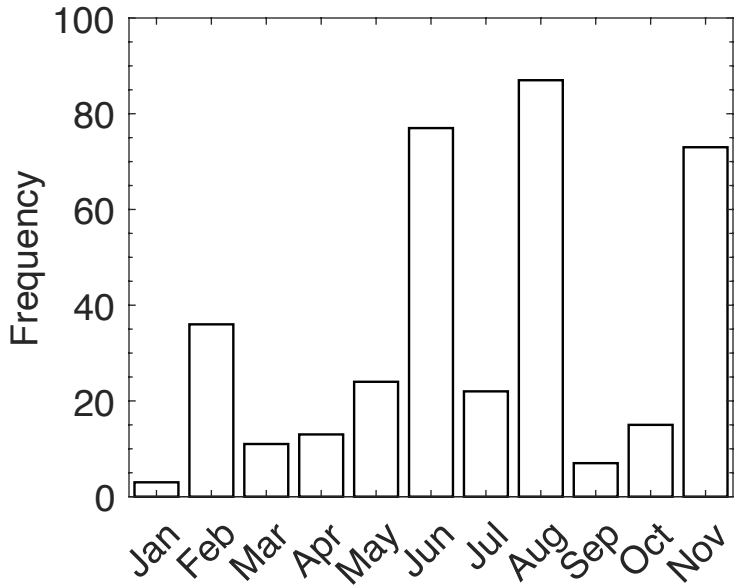

Training Set (N = 418)

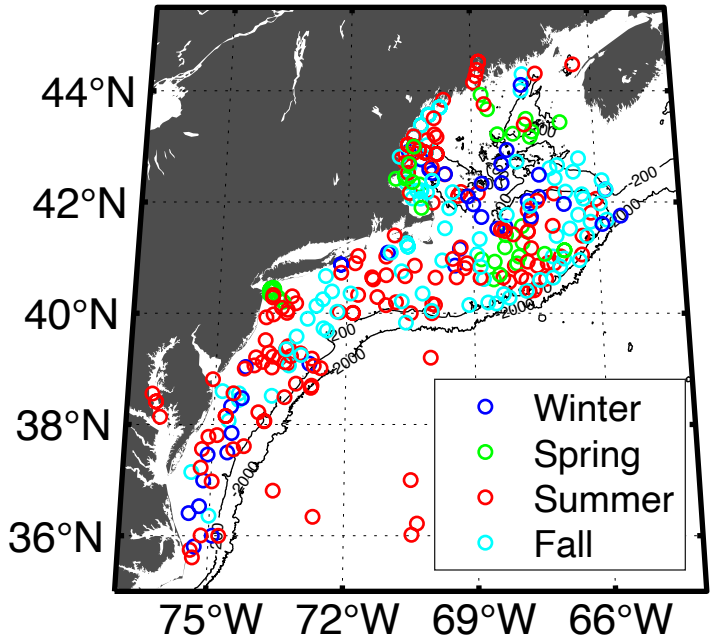

Validation Set (N = 368)

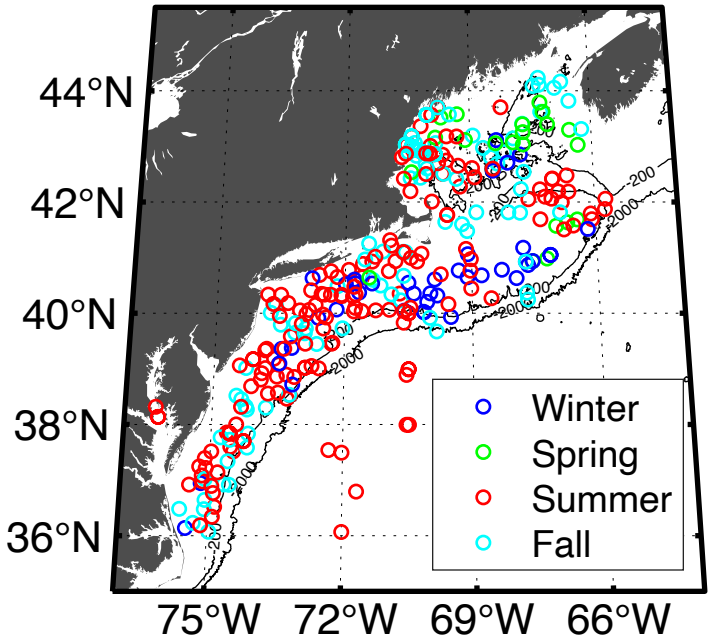

Table 2. Summary of *in situ* data sources. *N* denotes the number of samples (after QA), where the number in parentheses refers to the number of satellite match-ups. Citations for the individual data sets from SeaBASS are also provided.

Cruise/Experiment – P.I.(s)	*Year(s)*	*Month(s)*	*N, HPLC*	*N, $a_{ph}(\lambda)$*	*N, $a_{dg}(\lambda)$*
Impacts of Climate Variability on Primary Production and Carbon Distributions in the Middle Atlantic Bight and Gulf of Maine (CliVEC) – Mannino et al., 2009	2009-2012	Feb, May, Jun, Aug, Nov	424 (212)	182 (101)	153 (86)
NOAA Ecosystem Monitoring (EcoMon) – Mannino et al., 2013	2013, 2018	Feb, Aug, Nov	71 (41)	24 (18)	14 (9)
Optical and Nutrient Dependence of Quantum Efficiency (OnDeque3) – Marra et al., 2008	2008	Jul	26 (15)	0	0
Tara Oceans Expedition – Boss et al., 2009	2012	Jan, Feb	2	0	0
East Coast Ocean Acidification (ECOA-1) – Mannino et al., 2015	2015	Jun, Jul	37 (16)	0	0
LOBO timeseries – Roesler, 2009	2009	Mar	6	0	0
Western Gulf of Maine – Moore, 2006	2006-2009	All months	188 (68)	3	0
Ocean Color Cal Val (OCV) – Hooker et al., 2005	2007, 2009	May, Nov	16 (7)	0	0
COASTAL (C7) – Hooker, 2000	2008	Oct	6 (5)	5 (4)	6 (4)
Delaware and Chesapeake Bay Fluorescence – Chekalyuk, 2008	2008	May	1	0	0
2009oct_Chesapeake – Gould, 2009	2009	Oct	7 (3)	0	0
BIOCOMPLEXITY – Harding, 2001	2003	Aug	2 (1)	0	0
		Totals:	786 (368)	214 (123)	173 (99)

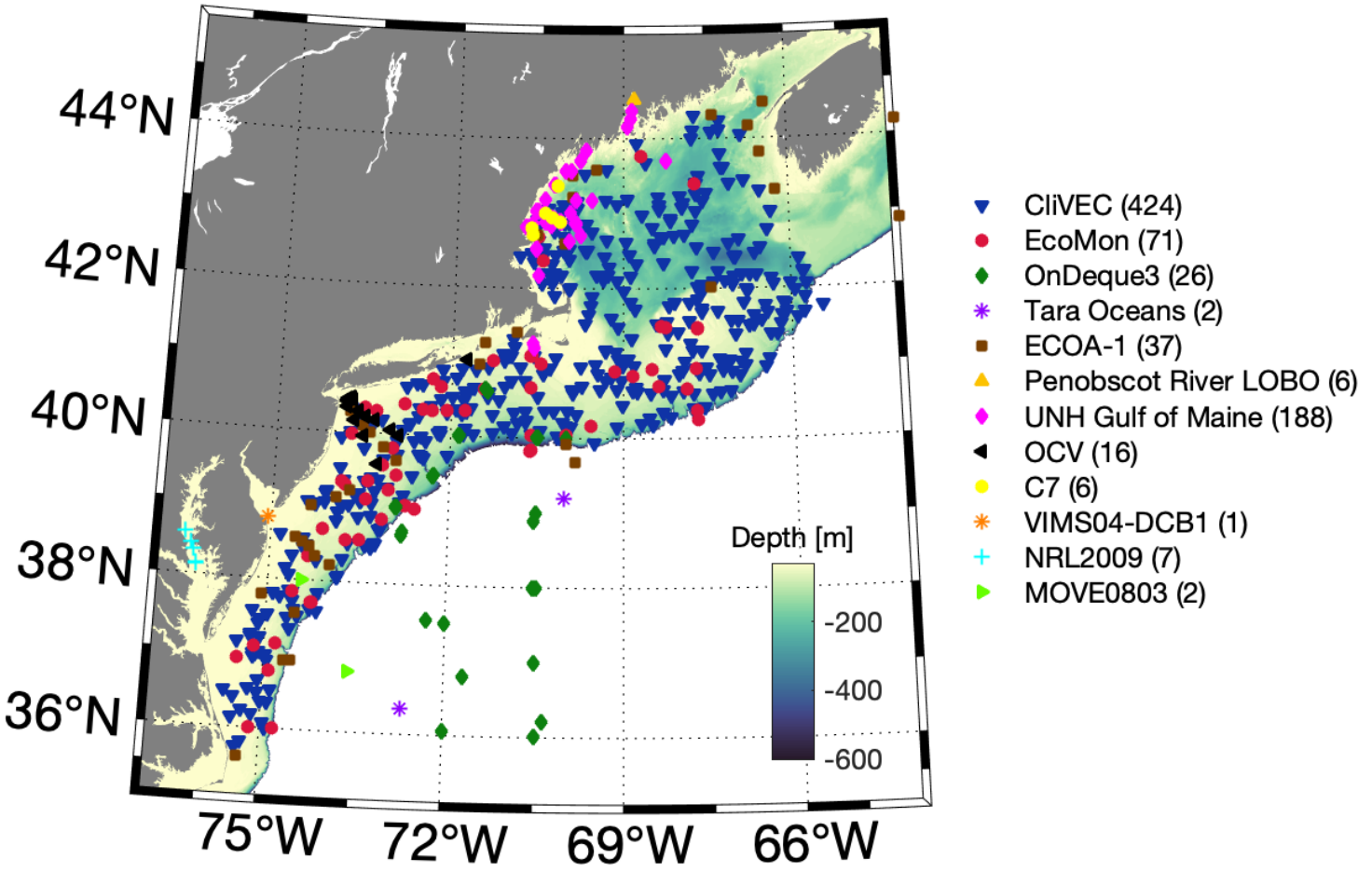

Table 3. Diagnostic pigments [***P***] and their associated taxonomic groups and attributed size classes, along with weighting coefficients [***W***] obtained from this study and previous studies. The number of data points and geographical regions of each study are also provided.

*Pigment [**P**]*	*Primary taxonomic group(s)*	*Attributed size class(es)*	*Weights [**W**]*			
			This study	*Uitz et al. (2006)*	*Brewin et al. (2015a)*	*Brewin et al. (2017)*
Fucoxanthin (P_1)	Diatoms	Micro/ nano	2.20	1.41	1.51	1.65
Peridinin (P_2)	Dinoflagellates	Micro	1.08	1.41	1.35	1.04
19'-Hex (P_3)	Prymnesiophytes	Nano	0.86	1.27	0.95	0.78
19'-But (P_4)	Pelagophytes	Nano	3.63	0.35	0.85	1.19
Alloxanthin (P_5)	Cryptophytes	Nano	-0.10	0.6	2.71	3.14
Total chlorophyll-b (P_6)	Prochlorophytes, Chlorophytes	Pico	1.21	1.01	1.27	1.38
Zeaxanthin (P_7)	Prochlorophytes, Cyanobacteria	Pico	0.99	0.86	0.93	1.02
		Number of data points	786	2419	5841	2239
		Geographic region	NES	Global	Global	North Atlantic

Table 4. Parameter values for the abundance-based models of Brewin et al. (2010) (Eqs. 9 and 10) and Hirata et al. (2011) (Eq. 16), obtained from this study and from previous studies.

Study	*Geographic region*	*Years*	*Parameters for Equations (9) and (10)*					
				$C^m_{pico,nano}$	C^m_{pico}	$D_{pico,nano}$	D_{pico}	
Brewin et al. (2010)	Atlantic	1997-2004	-	1.06	0.11	0.90	0.73	-
Brewin et al. (2015)	Global	1992-2012	-	0.77	0.13	0.94	0.91	-
Brewin et al. (2017)[a]	N Atlantic	1995-2015	-	0.82	0.13	0.87	0.73	-
Devred et al. (2011)	NW Atlantic	1996-2003	-	0.55	0.15	1.00	1.00	-
This Study	NES	2003-2018	-	0.81	0.15	0.78	0.54	-
			Parameters for Equation (16)					
			$b_{1,micro}$	$b_{2,micro}$	$b_{3,micro}$	$b_{1,pico}$	$b_{2,pico}$	$b_{3,pico}$
Hirata et al. (2011)[b]	Global	1995-2008	0.91	-2.73	0.40	-	-	-
Moore and Brown (2020)[c]	Atlantic	1997-2014	0.82	-1.33	0.39	1.41	2.82	1.72
This Study	NES	2003-2018	1.03	-1.68	-0.12	-3.45	0.67	2.29

[a] Refers to the *SST*-independent model from their study

[b] Hirata et al. (2011) used a different empirical formula to estimate picoplankton (Eq. 15; see their Table 2)

[c] Refers to coefficients derived using the DPA method [see Table 4 of Moore and Brown (2020)]

Parameter	Model	*in situ* parameterization set (N = 418)			*in situ* validation set (N = 368)		
		MAE	δ	*r*	*MAE*	δ	*r*
F_{micro} (C_{micro})	B-NES	0.18 (0.24)	0.01 (0.11)	0.56 (0.86)	0.19 (0.25)	0.01 (0.13)	0.44 (0.85)
	H-NES	0.18 (0.21)	0.00 (0.10)	0.55 (0.86)	0.19 (0.25)	0.01 (0.12)	0.46 (0.85)
	B10	0.19 (0.24)	-0.08 (0.00)	0.56 (0.86)	0.21 (0.26)	-0.08 (0.01)	0.44 (0.85)
	B15	0.18 (0.24)	-0.02 (0.05)	0.56 (0.86)	0.20 (0.25)	-0.04 (0.05)	0.45 (0.85)
	B17	0.18 (0.24)	-0.02 (0.07)	0.56 (0.86)	0.19 (0.25)	-0.02 (0.08)	0.44 (0.85)
	D11	0.19 (0.24)	0.03 (0.10)	0.55 (0.86)	0.19 (0.25)	0.02 (0.09)	0.45 (0.85)
	H11	0.19 (0.25)	-0.06 (-0.02)	0.56 (0.86)	0.21 (0.25)	-0.08 (-0.04)	0.44 (0.85)
	MB20	0.19 (0.24)	-0.06 (0.04)	0.55 (0.86)	0.20 (0.25)	-0.05 (0.06)	0.45 (0.85)
$F_{pico,nano}$ ($C_{pico,nano}$)	B-NES	0.18 (0.19)	-0.01 (0.06)	0.56 (0.67)	0.19 (0.20)	-0.01 (0.06)	0.44 (0.72)
	H-NES	0.18 (0.19)	-0.01 (0.06)	0.55 (0.67)	0.19 (0.19)	-0.01 (0.07)	0.46 (0.73)
	B10	0.19 (0.21)	0.08 (0.14)	0.56 (0.67)	0.21 (0.22)	0.08 (0.14)	0.44 (0.72)
	B15	0.18 (0.20)	0.03 (0.09)	0.56 (0.66)	0.20 (0.21)	0.04 (0.10)	0.45 (0.71)
	B17	0.18 (0.19)	0.02 (0.08)	0.56 (0.66)	0.19 (0.20)	0.02 (0.09)	0.44 (0.71)
	D11	0.19 (0.20)	-0.03 (0.01)	0.55 (0.65)	0.19 (0.20)	-0.02 (0.03)	0.45 (0.70)
	H11	0.19 (0.22)	0.06 (0.09)	0.56 (0.47)	0.21 (0.22)	0.08 (0.12)	0.44 (0.68)
	MB20	0.19 (0.20)	0.06 (0.14)	0.55 (0.67)	0.20 (0.20)	0.05 (0.13)	0.45 (0.73)
F_{nano} (C_{nano})	B-NES	0.15 (0.24)	0.00 (0.10)	0.37 (0.66)	0.17 (0.28)	0.01 (0.13)	0.12 (0.74)
	H-NES	0.14 (0.24)	-0.01 (0.10)	0.38 (0.67)	0.16 (0.28)	0.00 (0.12)	0.16 (0.72)
	B10	0.18 (0.29)	0.12 (0.25)	0.37 (0.66)	0.21 (0.32)	0.13 (0.27)	0.20 (0.74)
	B15	0.15 (0.25)	0.05 (0.16)	0.38 (0.66)	0.17 (0.29)	0.05 (0.19)	0.20 (0.74)
	B17	0.15 (0.25)	0.04 (0.15)	0.37 (0.66)	0.17 (0.28)	0.04 (0.18)	0.20 (0.74)
	D11	0.14 (0.24)	-0.04 (0.02)	0.39 (0.65)	0.16 (0.26)	-0.04 (0.05)	0.21 (0.73)
	H11	0.16 (0.26)	0.02 (0.09)	0.36 (0.55)	0.19 (0.30)	0.04 (0.15)	0.10 (0.73)
	MB20	0.17 (0.27)	0.07 (0.21)	0.26 (0.67)	0.18 (0.29)	0.06 (0.21)	0.18 (0.74)
F_{pico} (C_{pico})	B-NES	0.08 (0.21)	-0.01 (0.05)	0.61 (0.55)	0.10 (0.22)	-0.02 (0.04)	0.63 (0.54)
	H-NES	0.07 (0.21)	0.00 (0.09)	0.67 (0.53)	0.09 (0.21)	-0.01 (0.07)	0.73 (0.59)
	B10	0.08 (0.25)	-0.04 (-0.10)	0.63 (0.40)	0.10 (0.25)	-0.04 (-0.08)	0.71 (0.40)
	B15	0.08 (0.24)	-0.02 (-0.04)	0.63 (0.41)	0.10 (0.24)	-0.02 (-0.01)	0.70 (0.42)
	B17	0.08 (0.24)	-0.02 (-0.04)	0.63 (0.43)	0.10 (0.24)	-0.02 (-0.02)	0.70 (0.43)
	D11	0.09 (0.24)	0.01 (0.03)	0.63 (0.40)	0.10 (0.24)	0.02 (0.05)	0.71 (0.40)
	H11	0.09 (0.25)	0.05 (0.19)	0.62 (0.52)	0.11 (0.25)	0.04 (0.17)	0.64 (0.51)
	MB20	0.08 (0.24)	-0.01 (-0.02)	0.63 (0.34)	0.10 (0.24)	-0.01 (0.01)	0.70 (0.38)

Statistical metrics obtained when comparing the *in situ* pigment-based estimates of F_{size} and C_{size} from the parameterization and validation data sets with estimates from the abundance-based models shown in Figure 7. Statistical calculations were performed in linear space for F_{size} and $\log_{10}$ space for C_{size}. Metrics for C_{size} are shown in parentheses.

Table 6. Mean absolute error (*MAE*) and correlation coefficients (*r*) for F_{size} and C_{size} (values for C_{size} shown in parentheses) for the *SST*-dependent abundance-based models applied to the *in situ* parameterization and validation data sets. The percent change in the metrics when incorporating *SST* relative to the *SST*-independent models is included for reference. Percentages are rounded to the nearest 1%.

Parameter	*Model*	*in situ parameterization set (N = 418)*				*in situ validation set (N = 368)*			
		MAE	*% change with SST*	*r*	*% change with SST*	*MAE*	*% change with SST*	*r*	*% change with SST*
F_{micro} (C_{micro})	B-NES-*SST*	0.16 (0.21)	-11 (-13)	0.68 (0.89)	+21 (+3)	0.17 (0.24)	-11 (-4)	0.58 (0.87)	+32 (+2)
	B17-*SST*	0.19 (0.23)	+6 (-4)	0.54 (0.87)	-4 (+1)	0.20 (0.25)	+5 (0)	0.44 (0.85)	0 (0)
	MB20-*SST*	0.18 (0.23)	-5 (-4)	0.59 (0.83)	+7 (-3)	0.19 (0.24)	-5 (-4)	0.49 (0.86)	+9 (+1)
$F_{pico,nano}$ ($C_{pico,nano}$)	B-NES-*SST*	0.16 (0.17)	-11 (-11)	0.68 (0.75)	+21 (+12)	0.17 (0.18)	-11 (-10)	0.58 (0.77)	+32 (+6)
	B17-*SST*	0.19 (0.20)	+5 (+5)	0.54 (0.59)	-4 (-11)	0.20 (0.20)	+5 (0)	0.44 (0.72)	0 (+1)
	MB20-*SST*	0.18 (0.20)	-5 (0)	0.59 (0.56)	+7 (-16)	0.19 (0.19)	-5 (-5)	0.49 (0.73)	+9 (0)
F_{nano} (C_{nano})	B-NES-*SST*	0.13 (0.21)	-13 (-13)	0.55 (0.74)	+49 (+12)	0.15 (0.26)	-12 (-7)	0.39 (0.79)	+225 (+6)
	B17-*SST*	0.14 (0.24)	-7 (-4)	0.44 (0.66)	+19 (0)	0.16 (0.27)	-6 (-4)	0.29 (0.75)	+45 (+1)
	MB20-*SST*	0.16 (0.26)	-6 (-4)	0.28 (0.58)	+8 (-13)	0.16 (0.27)	-11 (-7)	0.18 (0.72)	0 (-3)
F_{pico} (C_{pico})	B-NES-*SST*	0.07 (0.19)	-13 (-10)	0.70 (0.64)	+15 (+16)	0.09 (0.20)	-10 (-9)	0.73 (0.62)	+16 (+15)
	B17-*SST*	0.08 (0.23)	0 (-4)	0.63 (0.46)	0 (+7)	0.09 (0.23)	-10 (-4)	0.73 (0.53)	+4 (+23)
	MB20-*SST*	0.08 (0.21)	0 (-13)	0.67 (0.53)	+6 (+56)	0.10 (0.22)	0 (-8)	0.72 (0.52)	+3 (+37)